Solvation thermodynamic properties from molecular dynamics on the terahertz time scale

Thermodynamische Eigenschaften von Lösungen aus molekularer Dynamik in der Terahertz-Zeitskala
Master-Thesis von Marvin Bernhardt
Tag der Einreichung: 16.12.2016

1. Gutachten: Prof. Dr. Nico van der Vegt
2. Gutachten: Dr. Cahit Dalgicdir

TECHNISCHE UNIVERSITÄT DARMSTADT

Fachbereich Chemie
Computational Physical Chemistry

Solvation thermodynamic properties from molecular dynamics on the terahertz time scale
Thermodynamische Eigenschaften von Lösungen aus molekularer Dynamik in der Terahertz-Zeitskala

Vorgelegte Master-Thesis von Marvin Bernhardt

1. Gutachten: Prof. Dr. Nico van der Vegt
2. Gutachten: Dr. Cahit Dalgicdir

Tag der Einreichung: 16.12.2016

Bitte zitieren Sie dieses Dokument als:
URN: urn:nbn:de:tuda-tuprints-60421
URL: http://tuprints.ulb.tu-darmstadt.de/id/eprint/6042

Dieses Dokument wird bereitgestellt von tuprints,
E-Publishing-Service der TU Darmstadt
http://tuprints.ulb.tu-darmstadt.de
tuprints@ulb.tu-darmstadt.de

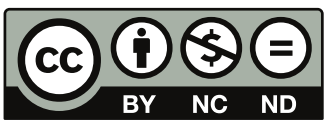

Die Veröffentlichung steht unter folgender Creative Commons Lizenz:
Namensnennung - Nicht kommerziell - Keine Bearbeitungen 4.0 International
https://creativecommons.org/licenses/by-nc-nd/4.0/deed.de

Contents

Abstract

The Two-Phase Thermodynamics (2PT) model describes an arbitrary system as a superpositon of a hard-sphere gas and a solid, enabling us to calculate the system's entropy, thereby making a connection from the dynamics to the thermodynamics. In this work the 2PT model is used to investigate effects of solutes on the dynamics and thermodynamics of water. The negative excess mixing entropy of water-methanol and water-ethanol mixtures are correctly predicted by the model and accounted to the lowered diffusion of the molecules in the mixture. Ethanol is found to lower the entropy of water more than methanol. A second system analyzed are aqueous solutions of sodium chloride. Increasing salt concentrations are shifting diffusional modes of water to oscillations and lower its entropy. Several problems of the 2PT model are pointed out which are related to the unphysical separation in two subsystems. Deviating separation schemes based on time separation, velocity separation and position separation are proposed and analyzed.

Deutsche Zusammenfassung

Molekulardynamiksimulationen sind eine wichtige Methode um Eigenschaften von Systemen vorherzusagen. Die thermodynamische Entropie ist eine solche Eigenschaft, die sich, im Gegensatz zur Energie, nicht als Zeitmittelwert berechnen lässt. Das Two-Phase Thermodynamics (2PT) Modell ist eine neuere Methode, um die Entropie direkt aus der Trajektorie zu berechnen. Dazu wird zunächst die Vibrations-Zustandsdichte (engl. density of states) berechnet, welche angibt, wie die kinetische Energie eines Systems über verschiedene Frequenzen verteilt ist. Sie hat die Form eines Spektrums mit Peaks bei den dominanten Oszillationen des Systems. Flüssigkeiten und Gase haben einen Beitrag bei der Frequenz null, welcher nicht einer unendlich langsamen Oszillation, sondern der Diffusion der Teilchen zugeordnet ist. Die grundlegende Idee des 2PT Modells ist es, die Zustandsdichte in zwei Beiträge zu zerlegen, einen diffusiven (gasartigen) und einen oszillierenden (feststoffartigen). Dazu wird der diffusive Beitrag durch ein Modellgas harter Kugeln modelliert. Der Anteil des Gases wird durch den Vergleich des Diffusionskoeffizienten mit einem theoretischen Referenzsystem nach der Enskog-Theorie vorhergesagt. Der übrige Teil der Zustandsdichte wird als Ensemble von harmonischen Oszillatoren betrachtet, für das sich die Entropie berechnen lässt. Die Gesamtentropie des Systems ist die Summe der Beiträge des Gases harter Kugeln und der Oszillatoren. Bei Systemen von Molekülen tragen Rotations- und Vibrationsfreiheitsgrade zusätzlich zur Entropie bei. Die Rotationszustandsdichte hat ebenfalls einen „diffusiven“ Anteil, der durch die freie Rotation verursacht wird. Das 2PT Modell separiert die Rotationsbewegung in starre Rotatoren und harmonische Oszillatoren und kann so auch die Entropie der Rotation abschätzen. Es ist ebenfalls für Mischungen definiert, wofür das Referenzsystem geändert wird.

Für diese Arbeit wurde das 2PT Modell implementiert und für zur Untersuchung von zwei Systemen verwendet. Anschließend wurden Probleme des Modells aufgezeigt und Verbesserungen entwickelt.

Als erstes System wurden Wasser-Methanol und Wasser-Ethanol Mischungen mit dem 2PT Modell untersucht. Die Exzessentropie von Alkohol-Wasser Mischungen is negativ, was meist durch molekulare Segregation erklärt wird. Das 2PT Modell sagt die negative Exzessentropie richtig vorher und kann darüber hinaus den Effekt auf die molaren Entropien der Komponenten zurückführen. In der Wasser-Methanol Mischung verliert hauptsächlich der Methanol Entropie. Wasser-Ethanol Mischungen zeigen ein differenzierteres Verhalten, bei dem sowohl Ethanol als auch Wasser Entropie verlieren. Alle Komponenten verlieren Rotationsentropie beim Mischen, dominant ist jedoch der Rückgang der Translationsentropie, welcher hauptsächlich durch einen verminderten Diffusionskoeffizienten erklärt wird. Die Ergebnisse sind zwar mit der molekularen Segregation vereinbar, eine genaue Aussage, welcher Prozess genau die Diffusion in der Mischung heruntersetzt, kann jedoch allein durch eine Untersuchung der Dynamik des Systems nicht getroffen werden.

Ein weiteres System, welches mit dem 2PT Modell untersucht wurde sind NaCl-Lösungen verschiedener Konzentrationen. Die Ionen haben nur einen sehr geringen Einfluss auf die Rotation der Wassermoleküle. Die Translation wird stark beeinflusst. Zum einen sinkt der Diffusionskoeffizient der Wassermoleküle. Des Weiteren verkleinert sich der Peak, welcher einer Biegebewegung der Wasserstoffbrückenbindungen zugeordnet wird. Die Energie wird zu einer Oszillation mit höherer Frequenz und damit niedrigerer Entropie verschoben. Nach dem Abziehen des Diffusionsanteils ergibt sich ein verändertes Bild. Die Verminderung des Peaks der Biegebewegung der Wasserstoffbrückenbindung ist verschwunden. Sie ist im 2PT Modell nur ein Überlagerungseffekt der verminderten Diffusion.

Neben den Analysen liegt ein Schwerpunkt der Arbeit darauf, die Probleme des 2PT Modells zu verstehen um es weiterzuentwickeln. Die wichtigste Einschränkung ist, dass die Separation der Teilchen in zwei Untersysteme physikalisch nicht verstanden werden kann, da jedes Teilchen in einem Fluid beide Eigenschaften haben muss. Das führt beispielsweise dazu, dass nur für ein Teil des Systems die Ununterscheidbarkeit der Teilchen angenommen wird. Die Zerlegung der Rotation in zwei Teile ist ebenfalls nicht physikalisch gelöst. Es wird die selbe Formel wie für die Translation verwendet, was einem Vergleich des „Rotations-Diffusionskoeffizienten“ mit dem Diffusionskoeffizienten des Referenzsystems entspricht. Diese Größen sind jedoch nicht vergleichbar. Auch wird im 2PT Modell die Rotation um alle drei Rotationsachsen eines Moleküls nicht getrennt behandelt. Das führt dazu, dass Effekte von Dipolen, die bestimmte Rotationen benachteiligen, vernachlässigt werden.

Es wurde eine Weiterentwicklung des 2PT Modells erarbeitet, bei der die Separation auf molekularer Ebene nachvollziehbar ist. Dazu wurde ein neuer Ansatz gewählt, bei dem die Separation der Bewegung der Moleküle in einen diffusiven und einen oszillierenden Teil erfolgt. Die Moleküle folgen einer langsamen, „weichen“ Trajektorie, welche der diffusiven Bewegung entspricht. Entlang dieses Weges oszillieren die Moleküle um den von der Diffusion vorgegebenen Weg. Es wurde gezeigt, dass dieser Ansatz mathematisch nicht mit dem ursprünglichen 2PT-Modell

vereinbar ist. Das führt zu einer neuen Interpretation der Teilsysteme. Jede der Bewegungskomponenten enthält einen Teil der kinetischen Energie, damit haben das gasartige und das oszillierende Teilsystem jeweils einen Teil der Gesamttemperatur. Eine Gewichtung mit einem idealen Gas und harmonischen Oszillatoren zur Berechnung der Entropie liegt nahe, wurde jedoch noch nicht getestet.

Zwei Schemata wurden vorgeschlagen um die Bewegungen direkt zu separieren, ohne Zuhilfenahme des Modells Harter Kugeln. Das erste teilt die Trajektorie jedes Moleküls in Stücke, jeweils an Stellen maximaler Geschwindigkeit. Die mittlere Geschwindigkeit während eines Teilstücks wird als diffusiver Beitrag interpretiert, der Rest als oszillierender. Diese Methode funktioniert für einige Systeme, filtert jedoch jeweils nur die Oszillation mit der höchsten Frequenz heraus. Bei Lennard-Jones Fluiden funktioniert das zuverlässig, flüssiges Wasser zeigt jedoch mehrere Oszillationsprozesse, von denen nur ein Teil herausgefiltert wird. Das zweite Schema benutzt einen Gauß-Filter um die Trajektorie zu glätten. Dabei wird die Breite der zum Glätten verwendeten gaußschen Glockenkurve solange erhöht, bis die geglättete Bewegung frei von Oszillationen ist. Dies wird durch eine monoton fallende Autokorrelationsfunktion angezeigt. Die geglättete Bewegung wird als diffusiver Beitrag interpretiert. Beide Schemata sind zu diskutieren, sie zeigen jedoch, dass es grundsätzlich möglich ist, die Bewegungen ohne weitere Annahmen zu separieren.

1 Introduction

An ordinary molecular dynamics simulation can offer a lot of insight into a system. However, the entropy and the free energy, two of the most interesting thermodynamic properties, are not directly accessible. The free energy difference between two states determines in which direction the system will evolve, if the states are connected by a path. This could be anything, the segregation of a mixture, a conformational change of a macromolecule or a chemical reaction. Free energy differences consist of two contributions: an entropy difference, that gives information about which state is favored because of phase space sampling, and an energy difference.

The energy can be computed for every conformation of molecules and therefore determined by taking the time average over a molecular dynamic trajectory. The entropy and free energy are not defined for a single configuration. They are rather defined from the partition function, which is a quantity averaged over all possible configurations, weighted with the Boltzmann factor. However, a direct sampling of position space of all molecules with a molecular dynamics (MD) trajectory is way beyond our possibilities.

The longest established methods for calculating free energies are thermodynamic integration and the Widom insertion method[1]. Thermodynamic integration connects two states of a system by a reversible path and calculates the free energy difference. For converging values many simulations along the path have to be performed and extensively sampled. The Widom insertion method works by randomly inserting a molecule into fixed conformations of a trajectory. From averaging over the Boltzmann factor with the insertion energy the chemical potential of the molecule can be computed. The result converges fast for small particles, but is difficult to converge for larger molecules.

An important method for the calculation of the entropy is based on correlation functions. The excess entropy of a fluid can be expressed as a series of multiparticle correlations functions[2]. The two-body entropy is the second term of the series, which is calculated from the radial distribution function. It can be taken as a estimate for the excess entropy of a fluid, because the higher terms of the series are small for systems of moderate densities[3].

In recent studies attempts have been made to calculate the absolute entropy directly from a MD trajectory. The quasiharmonic method gives an estimate of the absolute entropy of a system from the frequencies in the covariance matrix of the positional coordinates of molecules[4][5]. A notable improvement to that method is called permutation reduction[6]. The diffusional motions of particles were identified to be the main problem in the calculation of the entropy. The trajectory is altered in a way that every molecule stays close to its initial position. This is achieved by an algorithm that swaps the positions of the molecules until the sum of the distances of all molecules from their original position is minimal. Diffusion is therefore effectively suppressed.

The Two-Phase Thermodynamics (2PT) model is a recently developed method to calculate an estimate of the absolute entropy from a trajectory[7]. The method is based on the density of states (DoS) which gives information on how the kinetic energy of a system is distributed over its oscillating modes. The zero frequency value of the DoS is related to diffusion. Based on the observation that the DoS of a liquid has features of both the DoS of a gas and the DoS of a solid, the idea of the 2PT model is to treat a system of particles as two subsystems, a hard sphere gas and a set of harmonic oscillators. The gas is describing the diffusion, of the system and the harmonic oscillators account for the solid-like, oscillating movement of the particles. A fluidicity factor defines the percentage of the system that is gas-like. The fluidicity factor is defined to be the ratio of the diffusion coefficient of the system and the diffusion coefficient of a reference system according to Enskog theory. This definition gives the right limiting values. For a system with a diffusion coefficient of zero the fluidicity factor is zero. When the diffusion coefficient is equal to the prediction from Enskog theory, the fluidicity factor is one. The shape of a hard-sphere gas DoS is completely defined by the diffusion coefficient and the fluidicity factor. It is subtracted from the DoS of the system, to give the DoS of the oscillating subsystem. The entropy of the system is the sum of the contributions of the two subsystems. For weighting the oscillating modes the quantum-mechanical harmonic oscillator is used. The 2PT entropy usually converges within 50 ps to 100 ps, making it extremely cheap compared to the methods mentioned before.

For molecular systems the rotation and internal vibration contribute to the entropy. The rotation is split into two parts, freely rotating rigid bodies and harmonic oscillators[8]. Internal vibrations of small molecules are purely oscillating and usually have a small contribution to the entropy.

The method was extended to linear molecules[9], molecules with internal rotations[10], mixtures of atomic fluids[11] and mixtures of molecular fluids[12].

For a pure Lennard-Jones (LJ) fluid 2PT gives accurate values compared to the modified Benedict-Webb-Rubin equation of state over most parts of the phase diagram[7]. There have been two studies on the entropy of water. The first showed that 2PT underestimates the entropy of pure water compared to free energy perturbation and finite difference methods by 2 % to 5 %. The experimental value is underestimated by 3 % to 10 % depending on the water model[8]. In the second study entropies were calculated from trajectories of ab initio molecular dynamics with different density functionals. The resulting entropies are 18 % to 40 % under the experimental value, but the error is linked to the high tetrahedral ordering in the simulation[13] compared to the experiment.

A study on the molar entropies of 15 common solvents shows a correlation coefficient of 92 % with experimental values[14]. Gibbs free energies of mixtures of LJ fluids calculated with the 2PT model correlate reasonably with values from thermodynamic integration and the Widom insertion method[11]. However, only the Gibbs free energies and not the entropies are reported.

Recently an extension was proposed to the 2PT model for use with liquid metals[15]. It was found that the hard sphere gas DoS (a Lorentzian) overestimates the actual DoS in the high frequency region. By applying a memory function the gaseous DoS is fitted to behave correctly leading to increased accuracy of the resulting entropies. On that basis a model was developed to completely perform the separation into gas and solid contributions by fitting the velocity autocorrelation function (VAC) function, without the need to employ the hard sphere theory[16]. The resulting entropies are reasonable for some test systems, but the method has not been extensively tested yet.

The 2PT model is not only useful for calculation of the absolute entropy, it also gives insight into how dynamics contribute to that entropy. Several entropic effects have been explained with it. The spontaneous filling of carbon nanotubes with water was explained by the loss of the tetrahedral order of bulk water[17]. In a recent paper the 2PT model has been used to calculate the solvation free energy of positively charged spheres in water. The solutes had different radii and charge. The 2PT solvation entropy was found to cancel out the solvation energy for a charge of 0.4 e, independent of the radius, indicating a crossover from hydrophobic to hydrophilic behavior[18]. In another study the 2PT model has been used to investigate the dynamics and thermodynamics of water inside and at the surface of poly(amidoamine) dendrimers[19]. The water inside the dendrimer has a lower entropy due to confinement, promoting processes in which the water is released.

One system of interest in this work are water-alcohol mixtures, which experimentally show negative excess mixing entropies[20]. There are two descriptive theories in literature that explain the entropy loss. The “iceberg” model states that water molecules close to the hydrophobic alkyl group form patches of immobilized water[21]. Molecular segregation is an alternative mechanism, that explains the entropy loss by incomplete mixing on a molecular level[22][23].

A previous study investigated water-methanol mixtures with the 2PT model and found that the negative excess mixing entropy is correctly reproduced[12]. Comparing molar entropies, methanol was found to account for 75 % of the entropy loss, which contradicts the “iceberg” model, where the water molecules are responsible for the entropy loss. With the 2PT methodology the entropy loss was further split into its components: translational and rotational entropy, of which each has a diffusive and an oscillating contribution. The oscillating translational entropy was found to be responsible for most of the entropy loss.

Here molecular dynamics simulations of water-methanol and water-ethanol mixtures are analyzed with the 2PT model. The mixing entropy is compared to the experimental results. Comparing the effects of methanol and ethanol I find that ethanol significantly decreases the molar entropy of water more than methanol.

A second system of interest are solutions of ions. The self-diffusion coefficient of water is affected by ions[24] and they are known to effect the folding equilibria of proteins[25] and polymers[26]. This effect was originally explained by the influence of ions on the structure of water, i.e. the Hofmeister series[27].

The 2PT model gives insight into the dynamics and thermodynamics of a system and therefore is a useful tool to observe the influence ions have on water. A test system of sodium chloride aqueous solutions of different concentrations is analyzed in this work. The expected loss of molar entropy of the water is linked to changes in the translational and rotational dynamics. I find that sodium chloride mainly effects the translational entropy of water.

While being useful, the 2PT model itself has some aspects that appear unclear. The split of the particles into two subsystems, one a gas and one a solid needs to be understood on the molecular level, because the diffusive and oscillating contributions have to be present in every single particle equally. This is a major flaw of the method, since is not derived from the actual dynamics and therefore its accuracy can not be predicted. The empiric hard sphere formulas used have the same effect. They may give a good estimate, but the accuracy may be off in some cases.

The separation of the rotational degrees of freedom has to be questioned too. Firstly the same hard sphere formulas are used, without explanation why they should apply to the rotation of molecule. Secondly, the 2PT

model treats all three degree of freedom (DoF) equally, denying that they might be influenced differently from the forcefield.

Indistinguishability is another unclear aspect, because it is a contribution in the entropy of a gas ($-k\ln(N!)$). The entropy of a solid does not have that contribution, because there the atoms are assumed to be distinguishable. Does that mean, that in the 2PT model only the "gaseous" particles are assumed indistinguishable or all particles are "half-indistinguishable"? Especially for classical systems it is discussed in literature if particles have to be treated as indistinguishable objects[28][29].

To answer these questions new ways for separating the diffusive and oscillating motion are investigated. The motivation is initially to get rid of the empiric formulas that are present in hard sphere theory. Making the separation on a microscopic level by separating the velocities, gives new insight and a more physical modification of the 2PT model. The trajectory of each particle is interpreted as a superposition of a "smooth" diffusional motion and local oscillations. This is still a separation into subsystems, but the system is not split by the particle number but by the kinetic energy.

2 Theory

In the following sections the 2PT model will be explained starting from pure atomic systems, extending it to molecular fluids and finally mixtures. The vibrational density of states and its properties are the basis for that theory and will therefore be explained first.

2.1 Density of States

The vibrational DoS $S(\nu)$ gives a measure of how the kinetic energy of a system is distributed over its vibrational states with frequencies ν. For the case of N equal atoms $S(\nu)$ is a mass weighted sum over the spectral densities $s_{j,l}(\nu)$ of each translational DoF of N atoms

$$S(\nu) = \frac{2m}{kTN} \sum_{j=1}^{N} \sum_{l=1}^{3} s_{j,l}(\nu) \tag{2.1}$$

where m is the mass of the atom. j is counting over the N atoms and l over the three coordinates of each atom. The spectral density is the squared absolute value of the Fourier transform of the velocity of the corresponding DoF

$$s_{j,l}(\nu) = \lim_{\tau\to\infty} \frac{\left|\int_{-\tau}^{\tau} v_{j,l}(t) \exp^{-2\pi \mathrm{i} \nu t}\, dt\right|^2}{\int_{-\tau}^{\tau} dt} = \lim_{\tau\to\infty} \frac{1}{2\tau} \left| \int_{-\tau}^{\tau} v_{j,l}(t) \exp^{-2\pi \mathrm{i} \nu t}\, dt \right|^2 . \tag{2.2}$$

The prefactor $2/kT$ in Equation (2.1) is the normalizing factor for the kinetic energy of each DoF ($kT/2$). Deviating from literature I add $1/N$ as a prefactor, which makes the DoS an intensive property and simplifies its comparability. The integral over the DoS is therefore

$$\begin{aligned}
\int_0^\infty S(\nu) d\nu &= \frac{1}{2} \int_{-\infty}^{\infty} S(\nu) d\nu && \text{(2.3a)}\\
&= \frac{m}{kTN} \sum_{j=1}^{N} \sum_{l=1}^{3} \int_0^\infty s_{j,l}(\nu) d\nu && \text{(2.3b)}\\
&= \frac{m}{kTN} \sum_{j=1}^{N} \sum_{l=1}^{3} \int_0^\infty \lim_{\tau\to\infty} \frac{1}{2\tau} \left| \int_{-\tau}^{\tau} v_{j,l}(t) \exp^{-2\pi \mathrm{i} \nu t}\, dt \right|^2 d\nu && \text{(2.3c)}\\
&= \frac{m}{kTN} \sum_{j=1}^{N} \sum_{l=1}^{3} \lim_{\tau\to\infty} \frac{1}{2\tau} \int_{-\tau}^{\tau} (v_{j,l}(t))^2 dt && \text{(2.3d)}\\
&= \frac{m}{kTN} \sum_{j=1}^{N} \sum_{l=1}^{3} \overline{(v_{j,l}(t)^2)} = \frac{1}{kTN} \sum_{j=1}^{N} \sum_{l=1}^{3} kT && \text{(2.3e)}\\
&= 3. && \text{(2.3f)}
\end{aligned}$$

This reflects the three translational DoF of each atom. From Equation (2.3c) to (2.3d) Parseval's theorem is used, which states, that integration over the square of a signal's Fourier transform is equal to the integration over the signal's square itself.

As a result of the Wiener–Khinchin theorem the spectral density can be obtained from the VAC $c_{j,l}(t)$ of the velocity $v_{j,l}$

$$s_{j,l}(\nu) = \lim_{\tau\to\infty} \int_{-\tau}^{\tau} c_{j,l}(t) \exp^{-2\pi \mathrm{i} \nu t}\, dt. \tag{2.4}$$

From Equations (2.1) and (2.4) and the Green-Kubo relation for diffusion it follows, that the zero frequency value of the DoS is proportional to the diffusion constant

$$D = \frac{1}{3} \int_0^\infty c(t) dt = \frac{1}{6} \int_{-\infty}^{\infty} c(t) dt = \frac{1}{6} s(0) = \frac{kT}{12m} S(0). \tag{2.5}$$

2.2 Two-phase Thermodynamics Model

The DoS of an ideal solid has a vanishing zero frequency value because there is no diffusion. On the contrary, gases have a DoS where the zero frequency value is the maximum.

The idea of the 2PT model is to separate the DoS of a system in any state into two contributions. A sketch is given in Figure 2.1. The liquid DoS can be considered as a superposition of two contributions, referred to as diffusive (dif) and oscillating (osc) in this work.

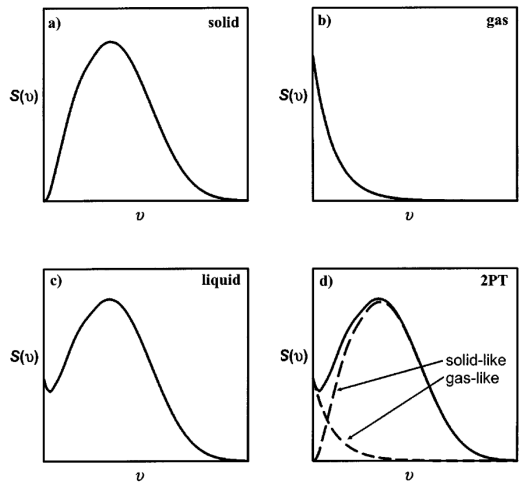

Figure 2.1: Typical densities of states for a) solid, b) gaseous and c) liquid state. The liquid DoS has features that can be reproduced by a combination of a gas-like and a solid-like DoS [7].

The separation of the DoS is assumed to be additive

$$S(\nu) = S^{\mathrm{dif}}(\nu) + S^{\mathrm{osc}}(\nu). \tag{2.6}$$

2.2.1 Separation with hard sphere theory

In the 2PT model the diffusive part is described by a hard sphere fluid, which is expected to have an exponentially decaying VAC function

$$c^{\mathrm{dif}} = \frac{3kT}{m}\exp(-\alpha t). \tag{2.7}$$

α is the Enskog friction constant. From Equations (2.1), (2.4) and (2.7) it follows, that the DoS of a hard sphere fluid is

$$S^{\mathrm{dif}}(\nu) = \frac{2m}{kTN}\sum_{j=1}^{fN}\lim_{\tau\to\infty}\int_{-\tau}^{\tau}\frac{3kT}{m}\exp(-\alpha t)\exp^{-2\pi \mathrm{i}\nu t}\,dt \tag{2.8a}$$

$$= 6f\lim_{\tau\to\infty}\int_{-\tau}^{\tau}\exp(-\alpha t)\exp^{-2\pi \mathrm{i}\nu t}\,dt \tag{2.8b}$$

$$= 6f\frac{2\alpha}{(2\pi\nu)^2+\alpha^2} \tag{2.8c}$$

$$= \frac{12f\alpha}{4\pi^2\nu^2+\alpha^2}. \tag{2.8d}$$

A **fluidicity factor** f is introduced in Equation (2.8a) and gives on a scale from 0 to 1 how much of the system is considered gas-like. This means that for the calculation the system's atoms are effectively divided into two groups or subsystems, a gas of fN hard spheres and $(1-f)N$ solidlike particles.

The integral of $S^{\mathrm{dif}}(\nu)$ over all positive frequencies is $3f$. The zero frequency value of $S^{\mathrm{dif}}(0) = s_0 = {}^{12f}/_{\alpha}$. With this the diffusive DoS can be rewritten to be dependent on s_0 instead of α

$$S^{\mathrm{dif}}(\nu) = \frac{s_0}{1 + \left(\frac{\pi s_0 \nu}{6f}\right)^2} \tag{2.9}$$

which is mathematically a Cauchy distribution.

As the oscillating part is not supposed to have a zero frequency value, s_0 is simply taken from the total DoS $s_0 = S(0)$. The only thing left to describe $S^{\mathrm{dif}}(\nu)$ and therefore the separation is the fluidicity factor f. It is set to the ratio of the diffusion coefficients of the system and a gas at zero pressure from the Chapman-Enskog theory

$$f = \frac{D(N,V,T)}{D_0^{\mathrm{HS}}(N,V,T,\sigma^{\mathrm{HS}})}. \tag{2.10}$$

Equation (2.10) gives the correct limiting values. When $D(N,V,T)$ is zero, f goes to zero, which makes sense because if there is no diffusion then all the motions are oscillating. If $D(N,V,T)$ converges to $D_0^{\mathrm{HS}}(N,V,T,\sigma^{\mathrm{HS}})$, f goes to one and the system behaves like a hard sphere fluid.

Another interpretation of why this is a meaningful definition of f is that a hard sphere gas at zero pressure can be thought of as having the maximum possible diffusion constant (at given temperature and number density). Additional forces, such as Pauli repulsion, London dispersion forces and electrostatics will all cause a reduction of the diffusion constant by introducing oscillations. Therefore the zero pressure gas is a suitable reference system.

We assume that all the diffusion comes from the fN hard sphere particles. Their diffusion constant therefore has to be ${}^1/_f$ times larger than the system's diffusivity

$$D^{\mathrm{HS}}(fN,V,T) = \frac{kT}{12mf} s_0 = D(N,V,T)/f. \tag{2.11}$$

The diffusion coefficient of a hard sphere fluid in the zero pressure limit is given by

$$D_0^{\mathrm{HS}}(N,V,T,\sigma^{\mathrm{HS}}) = \frac{3}{8} \frac{1}{\frac{N}{V}\sigma^{\mathrm{HS}2}} \left(\frac{kT}{\pi m}\right)^{1/2}. \tag{2.12}$$

This diffusivity is inversely related to the number of particles, therefore the diffusivity of a hard sphere gas with fN particles is ${}^1/_f$ times larger

$$D_0^{\mathrm{HS}}(fN,V,T,\sigma^{\mathrm{HS}}) = D_0^{\mathrm{HS}}(N,V,T,\sigma^{\mathrm{HS}})/f. \tag{2.13}$$

Enskog theory predicts the deviation of the diffusion constant of a hard sphere gas from the diffusivity in the zero pressure limit to be

$$D^{\mathrm{HS}}(fN,V,T) = D_0^{\mathrm{HS}}(fN,V,T,\sigma^{\mathrm{HS}}) \frac{4fy}{z(fy)-1}. \tag{2.14}$$

$z(fy)$ is the compressibility of the hard sphere gas and y the hard sphere packing fraction.

From Equations (2.10), (2.11), (2.13) and (2.14) f can be expressed as

$$f = \frac{4fy}{z(fy)-1} \tag{2.15}$$

Figure 2.2 outlines the relations of the four systems with their diffusion constants an how they are connected. The fluidicity factor f is defined as the relation of the actual system's and the reference system' diffusion coefficient. The hard sphere system does account for all the diffusion of the actual system, therefore its diffusivity is ${}^1/_f$ times larger. A second reference system is created with zero pressure and a density of ${}^{fN}/_V$. This system has a diffusion coefficient ${}^1/_f$ times larger then the first reference system. The relation of the diffusivities of the second reference system and the hard sphere system is known from Enskog theory.

The compressibility z is taken from the Carnahan-Starling equation of state

$$z(y) = \frac{1 + y + y^2 - y^3}{(1-y)^2} \tag{2.16}$$

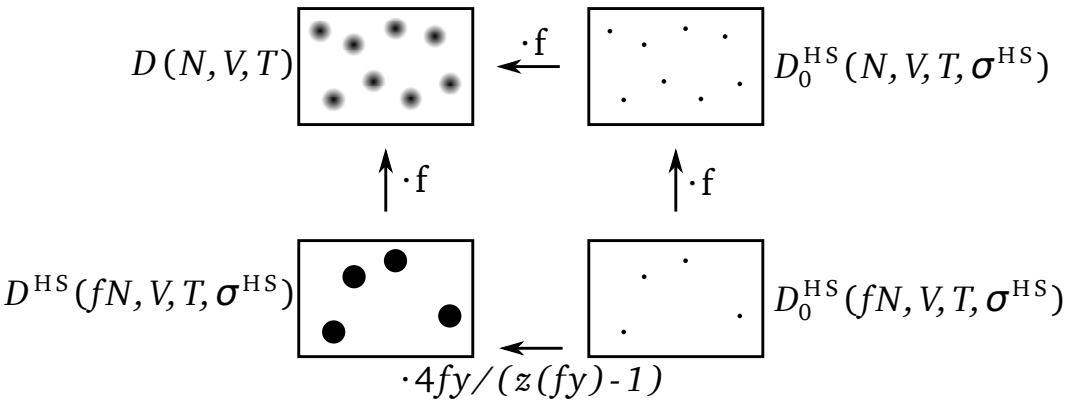

Figure 2.2: The four systems that are used to derive f. Arrows indicate the relation of the diffusion constant. Top left is the actual system as simulated with MD. Top right is a system at zero pressure with the same number of particles. f is defined to be the ratio of these system's diffusion constants. Also fN is the number of hard spheres that are used to account for the diffusivity in the real system (bottom left). On the bottom right is a zero pressure system with fN particles. Enskog theory predicts the deviation when going from zero pressure to a system with a certain packing fraction y.

and y is the hard sphere packing fraction

$$y = (\pi/6)\frac{N}{V}\sigma^{\mathrm{HS}}. \tag{2.17}$$

$D(N,V,T)$ can be obtained from the zero value of the density of states

$$D(N,V,T) = \frac{kT}{12m}s_0. \tag{2.18}$$

By solving Equations (2.10), (2.12) and (2.18) an expression for the packing fraction y is derived

$$y = \frac{f^{3/2}}{\Delta^{3/2}} \tag{2.19}$$

with the normalized diffusivity Δ, which is a unitless function of material properties and s_0

$$\Delta(N,V,T,m,s_0) = \frac{2s_0}{9}\left(\frac{\pi kT}{m}\right)^{1/2}\left(\frac{N}{V}\right)^{1/3}\left(\frac{6}{\pi}\right)^{2/3}. \tag{2.20}$$

Equations (2.15) and (2.19) can be combined to give an expression that can be used to calculate f directly

$$2\Delta^{-9/2}f^{15/2} - 6\Delta^{-3}f^5 - \Delta^{-3/2}f^{7/2} + 6\Delta^{-3/2}f^{5/2} + 2f - 2 = 0. \tag{2.21}$$

Therefore in order to obtain the fluidicity factor f one only needs to calculate Δ and solve Equation (2.21) numerically.

With s_0 and f the diffusive DoS $S^{\mathrm{dif}}(\nu)$ is defined and the oscillating part can be determined by subtracting the diffusive part from the total DoS

$$S^{\mathrm{osc}}(\nu) = S(\nu) - S^{\mathrm{dif}}(\nu). \tag{2.22}$$

The integral over the diffusive DoS is $3f$ and over the oscillating DoS $3(1-f)$.

2.2.2 Thermodynamic Properties from Weighting Functions

With the separation carried out, the system is treated as two independent subsystems. The oscillating part is treated as a set of harmonic oscillators with the total partition function

$$\ln Q = N \int_0^\infty S^{\mathrm{osc}}(\nu) \ln q_{\mathrm{HO}}(\nu)\ \mathrm{d}\nu \tag{2.23}$$

where $q_{\mathrm{HO}}(\nu)$ is the partition function of a single harmonic oscillator with frequency ν. If treated classically it is given by $q_{\mathrm{cHO}} = {}^1/_{\beta h \nu}$. For a quantum harmonic oscillator (qHO) the partition function is

$$q_{\mathrm{qHO}} = \frac{\exp(-\beta h \nu/2)}{1-\exp(-\beta h \nu)}. \tag{2.24}$$

Expressions for the energy, entropy and free energy arise

$$E^{\mathrm{osc}} = \left(\frac{\partial \ln Q}{\partial \beta}\right)_{N,V} = NkT \int_0^\infty S^{\mathrm{osc}}(\nu) W_E^{\mathrm{HO}}(\nu) \mathrm{d}\nu \tag{2.25a}$$

$$S^{\mathrm{osc}} = k \ln Q + kT \left(\frac{\partial \ln Q}{\partial \beta}\right)_{N,V} = Nk \int_0^\infty S^{\mathrm{osc}}(\nu) W_S^{\mathrm{HO}}(\nu) \mathrm{d}\nu \tag{2.25b}$$

$$A^{\mathrm{osc}} = -kT \ln Q = NkT \int_0^\infty S^{\mathrm{osc}}(\nu) W_A^{\mathrm{HO}}(\nu) \mathrm{d}\nu \tag{2.25c}$$

with the weighting functions for the quantum-mechanical case given by

$$W_E^{\mathrm{qHO}}(\nu) = \frac{\beta h \nu}{2} + \frac{\beta h \nu}{\exp(\beta h \nu)-1} \tag{2.26a}$$

$$W_S^{\mathrm{qHO}}(\nu) = \frac{\beta h \nu}{\exp(\beta h \nu)-1} - \ln(1-\exp(-\beta h \nu)) \tag{2.26b}$$

$$W_A^{\mathrm{qHO}}(\nu) = \ln \frac{1-\exp(-\beta h \nu)}{\exp(-\beta h \nu/2)}. \tag{2.26c}$$

Assuming the oscillating part as an ensemble of classic harmonic oscillators (cHOs) the weighting functions are

$$W_E^{\mathrm{cHO}}(\nu) = 1 \tag{2.27a}$$

$$W_S^{\mathrm{cHO}}(\nu) = 1 - \ln(\beta h \nu) \tag{2.27b}$$

$$W_A^{\mathrm{cHO}}(\nu) = \ln(\beta h \nu). \tag{2.27c}$$

The thermodynamic properties of the diffusive part are usually written down in terms of weighting functions. But as there is no dependence on the frequency ν, the integration over the diffusive DoS yields $3f$. One can therefore write

$$E^{\mathrm{dif}} = \frac{3}{2} f N k T \tag{2.28a}$$

$$S^{\mathrm{dif}} = f N S^{HS} \tag{2.28b}$$

$$A^{\mathrm{dif}} = f N \left(\frac{3}{2} kT - S^{HS} T\right). \tag{2.28c}$$

The hard sphere fluid entropy S^{HS} is given by

$$\frac{S^{HS}}{k} = \frac{S^{IG}}{k} + \ln(z(fy)) + \frac{fy(3fy-4)}{(1-fy)^2}. \tag{2.29}$$

S^{IG} is the entropy of an ideal gas given by the Sackur-Tetrode equation

$$S^{IG} = kN \ln\left(\frac{V}{N}\left(\frac{2\pi m k T}{h^2}\right)^{\frac{3}{2}}\right) + \frac{5}{2} kN. \tag{2.30}$$

The internal energy, entropy and free energy are obtained by summing the two contributions from Equations (2.25a) to (2.25c) and Equations (2.28a) to (2.28c), respectively

$$E = E_0 + E^{\text{osc}} + E^{\text{dif}} \tag{2.31a}$$

$$S = S^{\text{osc}} + S^{\text{dif}} \tag{2.31b}$$

$$A = E_0 + A^{\text{osc}} + A^{\text{dif}}. \tag{2.31c}$$

E_0 is the energy of the system obtained from the MD simulation, minus the kinetic energy of the diffusive part ($\frac{3}{2} f N k T$) and minus the (classical) kinetic and potential energy of the oscillating part ($(1-f)3NkT$)

$$E_0 = E^{\text{MD}} - 3NkT\left(1 - \frac{1}{2}f\right). \tag{2.32}$$

2.2.3 2PT for molecular systems

The 2PT model is also defined for systems of molecules[8]. The thermodynamic properties are separated into contributions from molecule's translation, rotation and vibration.

Translation

The molecules' translational DoS is defined by

$$S_{\text{trn}}(\nu) = \frac{2m}{kTM} \sum_{i=1}^{M} \sum_{k=1}^{3} \lim_{\tau\to\infty} \frac{1}{2\tau} \left| \int_{-\tau}^{\tau} v_{i,k}(t) \exp^{-2\pi \mathrm{i} \nu t}\, dt \right|^2 \tag{2.33}$$

where m is the mass of one molecule, $v_{i,k}(t)$ is the center of mass velocity of molecule i and M is the number of molecules. k indicates the x, y or z component of the velocity vector. The DoS is separated in the same fashion, as for atomic systems, with Equations (2.9) and (2.20) to (2.22), only with the molecule's mass. The resulting fluidicity factor is called f_{trn}. The contribution to the thermodynamic properties of the translation is calculated with the same functions as in Section 2.2.2 (again with the molecular mass).

Rotation

The molecules' rotational DoS is defined by

$$S_{\text{rot}}(\nu) = \frac{2}{kTM} \sum_{i=1}^{M} \sum_{l=1}^{3} \lim_{\tau\to\infty} \frac{I_i^l}{2\tau} \left| \int_{-\tau}^{\tau} \omega_i^l(t) \exp^{-2\pi \mathrm{i} \nu t}\, dt \right|^2 \tag{2.34}$$

where $\omega_i^l(t)$ is the angular velocity along the principal axis l of molecule i. I_i^l is the corresponding moment of inertia of the molecule. The integral of $S_{\text{rot}}(\nu)$ over all frequencies yields 3 associated with the three rotational DoF that each molecule possesses.

Originally the 2PT model was defined for non-linear molecules. In a later work carbon dioxide was investigated. It was found, that CO_2 is almost never linear during a molecular dynamics trajectory, making it possible to use the original formulas[9]. Actual linear molecules (diatomic molecules) have two rotational degrees of freedom and the principal axes are defined to be perpendicular to the bond, for which the directions are not defined. Therefore $\omega_i^l(t)$ is not well defined and Equation (2.34) cannot be used for linear molecules.

The rotation of a molecule has also a diffusive part, that can be present in gases, fluids and even some crystals, if the molecule can rotate freely to some degree. The rotational DoS is separated into diffusive and oscillating parts, with Equations (2.9) and (2.20) to (2.22). The resulting fluidicity factor is called f_{rot}. Energy and entropy contributions of the oscillating part of the rotation are given by Equations (2.25a) to (2.25c). For the diffusive part they are given by

$$E_{\text{rot}}^{\text{dif}} = f N \frac{3}{2} kT \tag{2.35a}$$

$$S_{\text{rot}}^{\text{dif}} = f N S^{RB} \tag{2.35b}$$

$$A_{\text{rot}}^{\text{dif}} = f N \left(\frac{3}{2} kT - S^{RB} T\right). \tag{2.35c}$$

S^{RB} is the rotational entropy of a rigid body

$$S^{RB} = k \ln\left(\frac{\pi^{1/2} e^{3/2}}{\sigma} \left(\frac{T^3}{\Theta_1 \Theta_2 \Theta_3} \right)^{1/2} \right) \tag{2.36}$$

with the rotational temperatures

$$\Theta_l = \frac{h^2}{8\pi^2 I_l k}. \tag{2.37}$$

σ is the rotational symmetry of the molecule.

Vibration

The molecules' vibrational DoS is defined by

$$S_{\text{vib}}(\nu) = \frac{2}{kTM} \sum_{i=1}^{M} \sum_{j=1}^{N_i} \sum_{l=1}^{3} \lim_{\tau \to \infty} \frac{m_{i,j}}{2\tau} \left| \int_{-\tau}^{\tau} v_{i,j,l}(t) \exp^{-2\pi \mathrm{i} \nu t} \, dt \right|^2 \tag{2.38}$$

where $m_{i,j}$ and $v_{i,j,l}(t)$ are the mass and velocity to atom j in molecule i (component l). The integral over the vibrational DoS yields $3N/M - 6$, which is equal the number of internal degrees of freedom of one molecule. Note that N is the total number of atoms and M the total number of molecules in the system.

For vibration it is assumed that there is no diffusional contribution, which means, that all internal movements are oscillations around the atom's relative positions. This is true only for molecules without internal rotations or other conformational changes such as ring flips. The 2PT model was also expanded to molecules that have rotating dihedrals [10]. Without that extension the 2PT model works only for molecules, where no internal rotations are present. The vibrational DoS is completely treated as harmonic motions ($S_{\text{vib}} = S_{\text{vib}}^{\text{osc}}$) and the energy and entropy contributions are given by Equations (2.25a) to (2.25c).

Sum of the Contributions

The thermodynamic properties of the system are obtained by summing over all the contributions

$$E = E_0 + E_{\text{trn}}^{\text{osc}} + E_{\text{trn}}^{\text{dif}} + E_{\text{rot}}^{\text{osc}} + E_{\text{rot}}^{\text{dif}} + E_{\text{vib}} \tag{2.39a}$$

$$S = \quad S_{\text{trn}}^{\text{osc}} + S_{\text{trn}}^{\text{dif}} + S_{\text{rot}}^{\text{osc}} + S_{\text{rot}}^{\text{dif}} + S_{\text{vib}} \tag{2.39b}$$

$$A = E_0 + A_{\text{trn}}^{\text{osc}} + A_{\text{trn}}^{\text{dif}} + A_{\text{rot}}^{\text{osc}} + A_{\text{rot}}^{\text{dif}} + A_{\text{vib}}. \tag{2.39c}$$

Here E_0 is the reference energy which will be given in Section 2.3.2.

2.2.4 2PT for Atomic Mixtures

2PT model is also generalized for atomic mixtures as derived in [11]. The DoS of each component $S_h(\nu)$ is calculated in the usual way from the velocities of the species with Equations (2.1) and (2.2). The densities of states are separated into the diffusive and oscillating contributions with Equations (2.20) and (2.21). In the definition of the dimensionless diffusion constant Δ there appears the number density $n = N/V$. For a mixture the inverse of the partial molar volume $\bar{V}_h$ is used, because the components share the total volume of the system. The equation for the dimensionless diffusion constant of component h is then

$$\Delta_h(\bar{V}_h, T, m_h, s_{0,h}) = \frac{2 s_{0,h}}{9} \left(\frac{\pi k T}{m_h} \right)^{1/2} \left(\frac{1}{\bar{V}_h} \right)^{1/3} \left(\frac{6}{\pi} \right)^{2/3}. \tag{2.40}$$

The number density also appears in the ideal gas entropy contribution in Equation (2.30), and is replaced with the inverse of the partial molar volume.

Three possibilities are given for obtaining the partial molar volume[11]. The first assumes, that all atoms have the same size and therefore the same molar volume, i. e. $\bar{V}_h = \bar{V} = V/N$. This breaks down in the case of different

sized atoms. The second accounts for the atom size using the Lennard-Jones parameter σ_h and gives reasonable results

$$\bar{V}_h = \frac{\sigma_h^3}{\sum_h x_h \sigma_h^3} \frac{V}{N}. \tag{2.41}$$

A third way uses Kirkwood-Buff theory to derive the partial molar volume from the radial distribution functions. This offers best results for Lennard-Jones fluids with different sized atoms[11]. But for obtaining well converged Kirkwood-Buff integrals long runs of large simulation boxes are needed. This somehow opposes the idea of 2PT to calculate the entropy from a relatively short trajectory.

For each component of the mixture h the thermodynamic properties are the sum of the oscillating and the diffusive contribution

$$E_h = E_{0,h} + E_h^{\text{osc}} + E_h^{\text{dif}} \tag{2.42a}$$
$$S_h = S_h^{\text{osc}} + S_h^{\text{dif}} \tag{2.42b}$$
$$A_h = E_{0,h} + A_h^{\text{osc}} + A_h^{\text{dif}}. \tag{2.42c}$$

The reference energy is calculated from the molecular dynamics energy for each component

$$E_{0,h} = E_h^{\text{MD}} - 3NkT(1 - f_h). \tag{2.43}$$

The properties of the system arise from the sum of the components

$$E_{\text{mix}} = \sum_h E_h \tag{2.44a}$$
$$S_{\text{mix}} = \sum_h S_h - kN \sum_h x_h \ln x_h \tag{2.44b}$$
$$A_{\text{mix}} = \sum_h A_h + kTN \sum_h x_h \ln x_h. \tag{2.44c}$$

The second term in Equation (2.44b) is the ideal mixing entropy. Without it there would be no mixing entropy, if two different fluids with similar forcefields mix, because the DoS would not change.

2.2.5 2PT for Molecular Mixtures

The 2PT moles was used to describe mixtures of molecules [12]. It is assumed that the compressibility of the system is, in good approximation, given by

$$z(y) = \sum_h x_h z_h(y) \tag{2.45}$$

the sum of the contributions of each component. Unfortunately the authors do not give further insights into their calculation but refer to the method of [11], which I described in the last section. It remains unclear which expression was used for the molar volume or how exactly the formulas for separating the rotational DoS are affected.

2.3 Problems of the 2PT Model

2PT model has proven to give good results and used for a variety of problems already. Yet there are some inconsistencies in it, that will be reported in this section.

2.3.1 Energy from the 2PT model

In [7] and [8] weighting functions for the energy and the free energy are defined. This may give the appearance, that the 2PT model offers an independent estimate of a system's energy. However by using the weighting function for the classical harmonic oscillator one finds

$$E = E_0 + E^{\text{osc}} + E^{\text{dif}} = E^{\text{MD}} - 3N(1-\frac{1}{2}f)kT + NkT\int_0^\infty S^{\text{osc}}(\nu)W_E^{\text{cHO}}(\nu)\mathrm{d}\nu + \frac{3}{2}fNkT \tag{2.46a}$$

$$= E^{\text{MD}} - 3N(1-\frac{1}{2}f)kT + 3(1-f)NkT + fN\frac{3}{2}kT \tag{2.46b}$$

$$= E^{\text{MD}} - 3N(1-\frac{1}{2}f)kT + 3N(1-\frac{1}{2}f)kT \tag{2.46c}$$

$$= E^{\text{MD}}. \tag{2.46d}$$

So independent of the fluidicity f, the resulting energy is just the energy from the MD simulation. Normally with the 2PT model the quantum mechanical weighting functions are used and it is noted in [12] that the 2PT model offers a quantum correction to the energy, but not an independent estimate. Therefore the model should mainly be used for the estimation of entropies.

2.3.2 Reference Energy in Molecular Fluids

In [8] a reference energy for a molecular fluid is given

$$E_0 = E^{\text{MD}} - kT3M(1-\frac{1}{2}f_{\text{trn}} - \frac{1}{2}f_{\text{rot}}). \tag{2.47}$$

However, it does not give the E^{MD} with classical weighting functions. For example in the case of $f_{\text{trn}} = f_{\text{rot}} = 1$ the reference energy would be equal to E^{MD}. By adding the energy from the diffusive and oscillating part, the resulting energy will be too large.

In order to keep the method consistent, E_0 is defined in a way, such that the energy from the classical 2PT model is equal E^{MD}

$$E^{\text{MD}} = E_0 + E_{\text{trn}}^{\text{osc}} + E_{\text{trn}}^{\text{dif}} + E_{\text{rot}}^{\text{osc}} + E_{\text{rot}}^{\text{dif}} + E_{\text{vib}} \tag{2.48a}$$

$$= E_0 + MkT\int_0^\infty S_{\text{trn}}^{\text{osc}}(\nu)W_E^{\text{cHO}}(\nu)\mathrm{d}\nu + \frac{3}{2}f_{\text{trn}}MkT + MkT\int_0^\infty S_{\text{rot}}^{\text{osc}}(\nu)W_E^{\text{cHO}}(\nu)\mathrm{d}\nu + \frac{3}{2}f_{\text{rot}}MkT \tag{2.48b}$$

$$+ MkT\int_0^\infty S_{\text{vib}}^{\text{osc}}(\nu)W_E^{\text{cHO}}(\nu)\mathrm{d}\nu \tag{2.48c}$$

$$= E_0 + 3(1-f_{\text{trn}})MkT + \frac{3}{2}f_{\text{trn}}MkT + 3(1-f_{\text{rot}})MkT + \frac{3}{2}f_{\text{rot}}MkT + M(3\frac{N}{M} - 6)kT \tag{2.48d}$$

$$= E_0 + 3MkT(1-\frac{1}{2}f_{\text{trn}}) + 3MkT(1-\frac{1}{2}f_{\text{rot}}) + (3N-6M)kT \tag{2.48e}$$

$$= E_0 + 3NkT - \frac{3}{2}MkT(f_{\text{trn}} + f_{\text{rot}}). \tag{2.48f}$$

Therefore the reference energy is

$$E_0 = E^{\text{MD}} - 3NkT + \frac{3}{2}MkT(f_{\text{trn}} + f_{\text{rot}}). \tag{2.49}$$

Note that the original definition of the reference energy is only wrong by a constant. Therefore the authors obtained the right values by only looking at energy differences. For linear molecules there is a similar derivation, which will not be given here, gives

$$E_0 = E^{\text{MD}} - 3NkT + \frac{3}{2}kTMf_{\text{trn}} + kTMf_{\text{rot}}. \tag{2.50}$$

As this definition is strongly dependent on the available DoFs the formula changes with intramolecular constraints. For rigid nonlinear molecules ($E_{\text{vib}} = 0$) the reference energy becomes

$$E_0 = E^{\text{MD}} - 3MkT(2-\frac{1}{2}f_{\text{trn}} - \frac{1}{2}f_{\text{rot}}). \tag{2.51}$$

2.3.3 Classic and Quantum Mechanic Model

In the original 2PT model there are two ways of treating the oscillations: classically and quantum mechanically[7] also called 2PT(C) and 2PT(Q). Later it became normal to use the quantum mechanical weighting functions and the results were compared with free energies from thermodynamic integration, particle insertion and experiment[9][10][8].

It makes sense to compare experimental results with 2PT(Q), because molecules *are* quantum mechanical objects in the real world. But TI and particle insertion methods have no notion of quantum effects.

As an example consider the free energy difference between two harmonic oscillators with different frequencies. 2PT(C) gives the expected classical free energy difference of $k\ln(\beta h\nu_2/\nu_1)$. The same result would be expected from a free energy method. But with 2PT(Q) the free energy difference is

$$\Delta A = \ln\frac{1-\exp(-\beta h\nu_2)}{\exp(-\beta h\nu_2/2)} - \ln\frac{1-\exp(-\beta h\nu_1)}{\exp(-\beta h\nu_1/2)}. \tag{2.52}$$

The error can be very small, depending on how large ν is, but in general the outcome is not the same.

Therefore the results of TI, particle insertion or other free energy methods should be compared with 2PT(C) rather than with 2PT(Q).

2.3.4 Moment of Inertia of Flexible Molecules

In the calculation of the rotational DoS in Equation (2.34) the moments of inertia I_i^l are taken as the constants. They can be obtained from the equilibrium structure of a single molecule. If the molecule is flexible I_i^l is no longer a constant but a function of time and $I_i^l(t)$ should go inside the Fourier transform

$$S_{\text{rot}}(\nu) = \frac{2}{kTM}\sum_{i=1}^{M}\sum_{l=1}^{3}\lim_{\tau\to\infty}\frac{1}{2\tau}\left|\int_{-\tau}^{\tau}\sqrt{I_i^l(t)}\omega_i^l(t)\exp^{-2\pi i\nu t}\,dt\right|^2. \tag{2.53}$$

For this definition one can show that the integral over all frequencies of the rotational DoS gives 3

$$\begin{aligned}
\int_0^\infty S_{\text{rot}}(\nu)d\nu &= \frac{1}{2}\int_{-\infty}^{\infty} S_{\text{rot}}(\nu)d\nu && \text{(2.54a)}\\
&= \frac{1}{kTM}\sum_{i=1}^{M}\sum_{l=1}^{3}\int_0^\infty \lim_{\tau\to\infty}\frac{1}{2\tau}\left|\int_{-\tau}^{\tau}\sqrt{I_i^l(t)}\omega_i^l(t)\exp^{-2\pi i\nu t}\,dt\right|^2 d\nu && \text{(2.54b)}\\
&= \frac{1}{kTM}\sum_{i=1}^{M}\sum_{l=1}^{3}\lim_{\tau\to\infty}\frac{1}{2\tau}\int_{-\tau}^{\tau} I_i^l(t)(\omega_i^l(t))^2 dt && \text{(2.54c)}\\
&= \frac{1}{kTM}\sum_{i=1}^{M}\sum_{l=1}^{3}\overline{I_i^l(t)(\omega_i^l(t))^2} = \frac{1}{kTM}\sum_{i=1}^{M}\sum_{l=1}^{3} kT && \text{(2.54d)}\\
&= 3. && \text{(2.54e)}
\end{aligned}$$

This does not work, if the moment of inertia is treated as a constant. Therefore when using the 2PT model for flexible molecules Equation (2.53) should be used.

2.3.5 Separation of the Rotational DoS

Using Hard Sphere Theory

The separation of the rotational DoS is performed with the same equations that are used for the translational DoS: Equations (2.20) and (2.21). These formulas were derived by comparing the systems diffusion coefficient to a reference systems diffusion coefficient. By applying them in the same way on Rotation corresponds to a comparison of the rotational diffusion coefficient of the molecules with the translational diffusion coefficient of the reference system. These properties are to my knowledge not directly related, which makes the separation unphysical. One

could argue, that Equation (2.21) is a general expression, that is independent from the actual type of motion. This seems unlikely, since the formula of Δ includes a particle's mass, but nothing about its moment of inertia.

When looking at data from simulations, one can see unexpected behavior in some cases. As an example one can take a look at the translational and rotational DoS of steam as shown in Figure 2.3. 2PT theory gives a fluidicity factor for translation of $f_{\text{trn}} = 0.98$. The actual DoS is not exactly, but reasonably reproduced, by what hard sphere (HS) theory predicts. As a result, the oscillating part becomes partly negative. This is unphysical, but the derivation is small, so no big influence is expected.

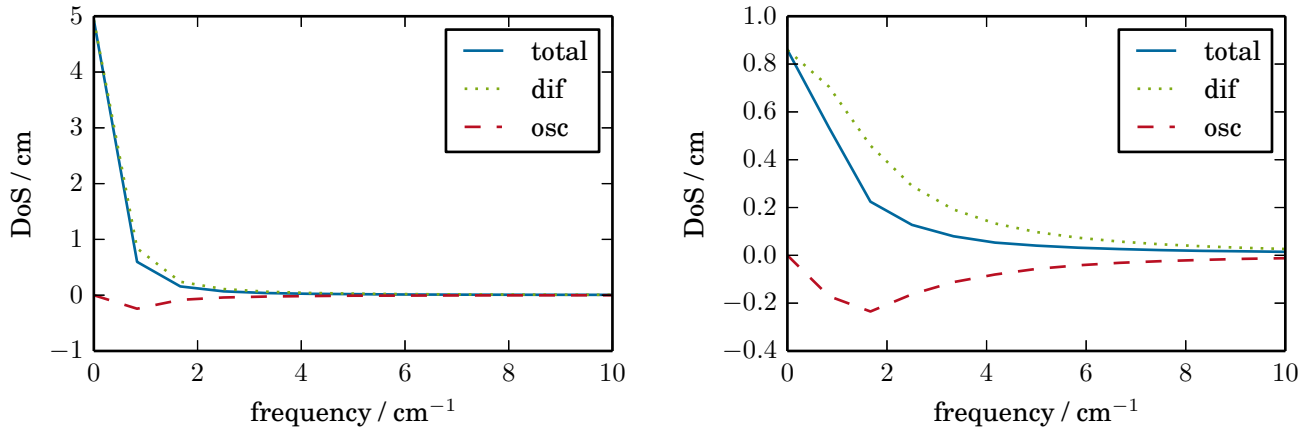

(a) Translational DoS separated in a diffusional and an oscillating part with $f_{\text{trn}} = 0.98$.

(b) Rotational DoS separated in a diffusional and an oscillating part with $f_{\text{rot}} = 0.80$.

Figure 2.3: The translational and rotational DoS of water vapor at 500 K and $\rho = 2.5\,\text{kg}\,\text{m}^{-3}$ with the separation according to the 2PT model. The prediction of the diffusive part of the translational DoS is a bit larger than the total DoS. The oscillating DoS becomes partially negative. The same effect is present in the rotational DoS, but stronger.

The rotational DoS in Figure 2.3b is not well reproduced by hard sphere theory. The fluidicity is $f_{\text{rot}} = 0.80$ so the diffusive part is expected to contribute to the total DoS. It is however larger than the total DoS in the range from $0\,\text{cm}^{-1}$ to $10\,\text{cm}^{-1}$. Therefore, the oscillating part has a large negative part. Low frequency harmonic oscillators have a large entropy and therefore this will strongly influence the total rotational entropy. Note that still the integral over the diffusive DoS is $3f_{\text{rot}}$ and over the oscillating $3(1-f_{\text{rot}})$, because there is a wide maximum of $S^{\text{rot}}(\nu)$ around $100\,\text{cm}^{-1}$ which is not shown in the plot.

Rotation around the Three Principal Axes

The rotational DoS can be further separated into contributions from rotations around the three principal axis of the molecule

$$S^{l}_{\text{rot}}(\nu) = \frac{2}{kTN}\sum_{i=1}^{M}\lim_{\tau\to\infty}\frac{I^{l}_{i}}{2\tau}\left|\int_{-\tau}^{\tau}\omega^{l}_{i}(t)\exp^{-2\pi\mathrm{i}\nu t}\,dt\right|^{2}. \tag{2.55}$$

Here l is the index of the principal axis which i will denote as a, b and c, in ascending order of the moment of inertia. In Figure 2.4 the situation is shown for water.

An interesting thing to note is, that the rotation around axis b, which has the medium moment of inertia, has the largest zero frequency value and therefore the highest rotational diffusivity. This is the expected behavior, accounting for the water structure, because the dipole of water molecule is along that axis and does not change with the rotation around it. The electrostatic hindrance is low and the molecule's orientation around axis b "diffuses" most even though it has only the second lowest moment of inertia.

2PT model treats the rotations around the three principal axis without distinguishing them, by working only with the total DoS. The entropy for the diffusive part is calculated from a rigid rotor with three rotational temperatures. That model assumes that all three rotations contribution to the entropy, dependent only on the moment of inertia. However as shown for water, the diffusivity is not only influenced from the moment of inertia, but also the force-field. Therefore I highly suggest, that whatever method is used to separate oscillating from diffusive motions, it

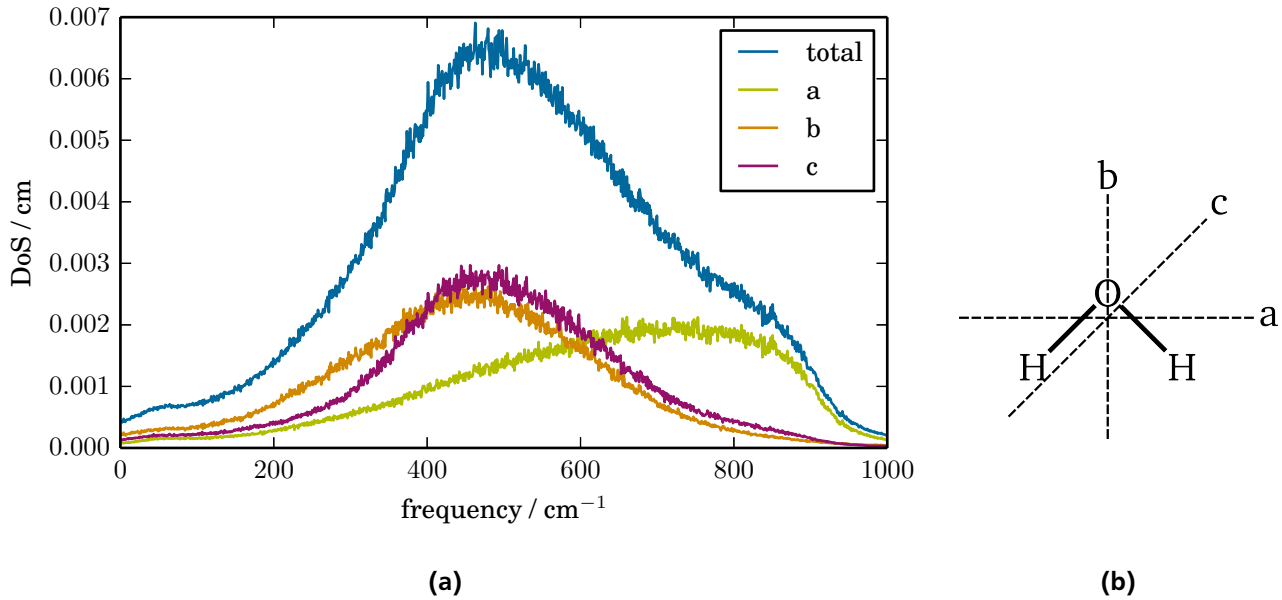

(a) (b)

Figure 2.4: (a) Rotational DoS of SPC/E water at $273\,\mathrm{K}$ and $\rho = 999.8\,\mathrm{kg\,m^{-3}}$. The total DoS is the sum of the contributions from rotations around the three principal axes, which are shown in (b). The order of the moments of inertia is $I_a < I_b < I_c$. The order of the zero frequency values is $S_a(0) < S_c(0) < S_b(0)$.

should be carried out on the three rotational degrees of freedom separately. If Equation (2.21) would be suitable for this job (which it isn't, as i showed in the fist part of this section), then the obvious solution would be to apply it to each DoS and use the entropy of a single rotational DoF with the given moment of inertia.

With these two general problems of the 2PT model regarding rotation its generality has to be questioned.

3 Computational Details

3.1 Molecular Dynamics

All simulations have been performed with the GROMACS [30] package (version 5.1.4). For the water-alcohol systems cubic boxes have been filled with randomly positioned OPLS-AA[31] alcohol and SPC/E[32] water molecules up to a total count of 500 molecules. The aqueous solutions of sodium chloride have been prepared in a similar way, by randomly inserting 10000 SPC/E water molecules and additional number of sodium and chloride OPLS ions in a box.

The systems were compressed to give the target pressure of 1 bar with a 50 ps run with a Berendsen barostat (time constant 0.2 ps). This was followed by an equilibration run of 100 ps to 200 ps and the production run of 200 ps, both with the same parameters. For temperature coupling the Nosé-Hoover thermostat (time constant 1 ps) and for pressure coupling the Parinello-Rahman barostat (time constant 10 ps) was used. Reference temperature is 300 K. Long range Coulombic interactions were calculated by using the particle-particle particle-mesh Ewald method with a local cutoff of 0.95 nm. The time integration was performed with the standard GROMACS leap frog integrator and a time step of 1 fs.

Position and velocity were written to a trajectory file every 4 fs. This high frequency output is needed for computing the DoS. Each simulation was performed four times with different starting conformations in order to obtain a rough estimate of the statistical precision of the results.

3.2 Two-Phase Thermodynamic Model

The calculation of the DoS for atomic systems is straightforward by reading the velocities from the trajectory file and calculating the absolute squared of the Fourier transform for every DoF. The discrete Fourier transform was computed by the numpy.fft tools[33] when working in python or FFTW[34] in compiled C programs.

For molecules the velocity has to be separated into translation, rotation and internal vibration. This is done at every step of the trajectory for every molecule. The translational velocity of a molecule v_i is calculated from the center of mass movement of the molecule's atoms

$$v_i^{\mathrm{trn}} = \frac{\sum_{j=1}^{N_i} m_{i,j}\, v_{i,j}}{\sum_{j=1}^{N_i} m_{i,j}}. \tag{3.1}$$

N_i is the number of atoms in molecule i and $m_{i,j}$ is the mass of atom j in molecule i.

The angular velocity vector $\vec{\omega}$ is calculated from the inverse of the moments of inertia tensor times the angular momentum $\vec{L}$

$$\vec{\omega}_i = \mathbf{I}_i^{-1} \cdot \vec{L}_i. \tag{3.2}$$

The coordinates of $\vec{\omega}_i$ are Cartesian coordinates. In order to obtain the angular velocities along the molecules principal axis l, which are needed by Equation (2.34), the eigenvectors $\vec{e}_l$ of the moment of inertia tensor are used

$$\omega_{i,l} = \frac{1}{I_{i,l}} \vec{L}_i \cdot \vec{e}_l. \tag{3.3}$$

This definition gives rise to a smaller problem in the computation of $\omega_{i,l}$ because $\vec{e}_l$ can point in both direction of the principal axis. That gives the angular velocity a random sign, making it unusable for Fourier analysis.

There are at least two easy ways to treat this. The first would be to compare the eigenvector with itself from one time step before. The second is to define auxiliary vectors within the molecule, that point in the same direction as the principal axes. The eigenvector is checked to have a positive dot product with its auxiliary vector. If this is the case, it means that the eigenvector is pointing in the same direction as the auxiliary vector. If it is negative, the eigenvector is multiplied by -1, thereby ensuring it always points in the same direction. The code I wrote uses the latter solution. For example for water the first auxiliary vector is connecting hydrogen atoms one and two. The

second vector points from the center of mass to the oxygen atom and the third is the cross product of the first two. The order is of ascending moment of inertia.

The internal vibrational velocities is the remainder of the atom's velocity, minus the center of mass movement and minus the velocity from the rotation of the molecule

$$v_{i,j}^{\text{vib}} = v_{i,j} - v_i^{\text{trn}} - \vec{\omega}_i \times \vec{r}_j. \tag{3.4}$$

The separation of the DoS is done by solving Equation (2.21) numerically, for which the Brent routine from the scipy python package[35] was used.

The partial molar volumes for the calculation of the 2PT entropy is determined from the LJ parameter σ for the NaCl solution. For the water-alcohol mixtures this is difficult, because the alcohols are molecules with several interaction sites. Therefore for those systems the simpler and possibly poorer approximation $\overline{V}_h = V/N$ was used.

Also the entropy of all internal modes was ignored, because the OPLS/AA methanol and ethanol have internal rotations, which are not yet covered by my code, see Section 2.2.3. SPC/E water is stiff and therefore has no internal vibrations.

4 Results and Discussion

In this chapter the results of my calculations are presented. First a pure water system is investigated, then water-alcohol mixtures and solutions of sodium chloride will be discussed.

4.1 Pure Water

Pure water is the reference for the water-alcohol mixtures and the NaCl solutions. It is therefore a good check for functionality of the model and starting point for later comparisons. The translational and rotational density of states are shown in Figure 4.1.

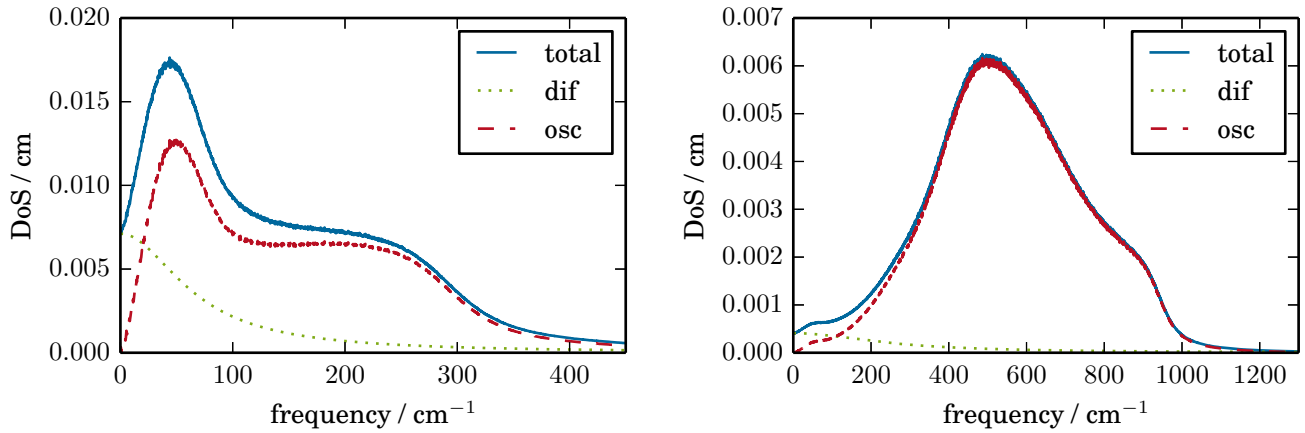

Figure 4.1: The (a) translational and (b) rotational DoS of pure SPC/E water. Also shown is the separation in diffusive and oscillating contributions. The translational DoS has a dominant peak at 50 cm^{-1} and a shoulder at 220 cm^{-1}. The rotational DoS has a peak at 500 cm^{-1} and two shoulders, one at 50 cm^{-1} and one at 900 cm^{-1}.

The translational DoS of water shows two peaks. The higher frequency peak at around 220 cm^{-1} can be assigned to the oscillations of two water molecules in the minimum of the LJ potential by a quick estimate of the frequency[36]

$$\omega = \sqrt{\frac{72\epsilon}{\mu\,(2^{1/6}\sigma)^2}} = \sqrt{\frac{72 \cdot 0.65\,\mathrm{kJ\,mol^{-1}}}{9\,\mathrm{u}\,(2^{1/6}\,3.166\,\text{Å})^2}} = 6.42\,\mathrm{THz} = 214\,\mathrm{cm^{-1}}. \tag{4.1}$$

This peak is not visible in the rotational spectrum, which makes sense, because the oscillation of two water molecules against each other does not alter their orientation. The other peak at around 50 cm^{-1} is often related to a bending of hydrogen bonds, or recently to an umbrella like motion of two water tetrahedrons[37]. This peak is therefore visible in the rotational DoS. Furthermore the rotational DoS shows a peak at 500 cm^{-1} and a shoulder at around 900 cm^{-1}. These can be dissected into contributions from the three rotational axes, which was already shown in Section 2.3.5. Both spectra have a zero frequency contribution, which means that water molecules diffuse and their orientation is not trapped.

The values for the entropy computed from the 2PT method are shown in Table 4.1. For comparison with literature in this case SPC water was used in an NVT simulation with a mass density of 1 g cm^{-3}.

The values calculated deviate from the literature value more than can be explained from statistical spread. However the relative deviation is smaller than 1 % and is most likely the result of small differences in the molecular dynamics procedure.

As an additional verification the entropy of liquid SPC water along the vapor-liquid equilibrium curve has been calculated. The resulting entropies are shown in Figure 4.2.

Table 4.1: Comparison of entropies for SPC water calculated with the 2PT method.

Entropy in $\mathrm{J\,K^{-1}\,mol^{-1}}$	S	S_{trn}	S_{rot}
this work (298 K)	65.513 ± 0.009	53.408 ± 0.008	12.091 ± 0.001
Lin et al.(298 K)[8]	65.09 ± 0.13	53.05 ± 0.14	12.03 ± 0.03
exp. (298.15 K)[38]	69.95 ± 0.03	–	–

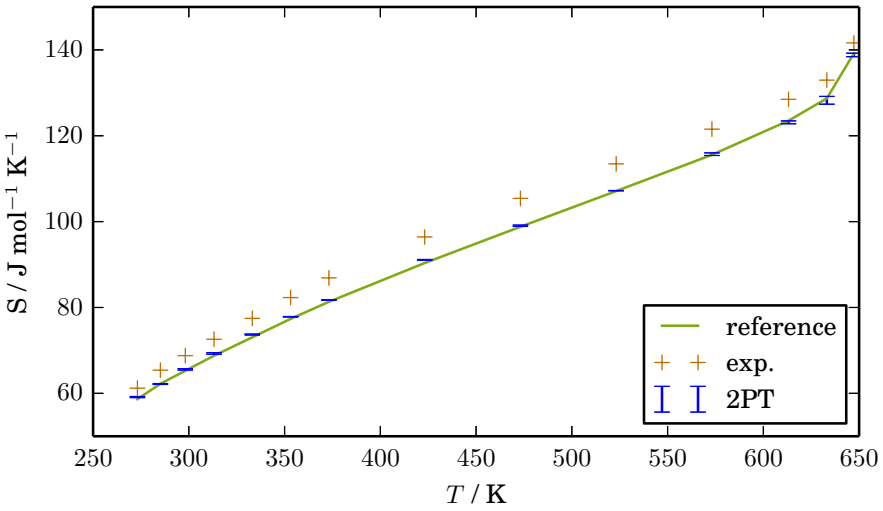

Figure 4.2: Comparison of the entropy of liquid SPC water along the vapor-liquid equilibrium curve with reference and experimental values[8]. The reference values are well reproduced. The values show the same trend as the Experiment, but the entropy is underestimated by $3\,\mathrm{kJ\,mol^{-1}}$ to $10\,\mathrm{kJ\,mol^{-1}}$

The reference line is well met and shows the precision of the 2PT method and also, if one accounts the offset to the forcefield, that general experimental trends are reproduced.

4.2 Water-Alcohol Mixtures

Water-methanol mixtures have been examined with the 2PT model before[17]. The investigations of water-ethanol mixtures are new. Mixtures with a mole fractions of methanol and ethanol of 0, 0.05, 0.1, 0.2, 0.4, 0.6, 0.8, 0.9, 0.95, 1 are analyzed.

4.2.1 Dynamics

By comparing the DoS one can see how mixing affects the dynamics of the different components. In Figure 4.3 the translational and rotational densities of states of the components in water-methanol and water-ethanol mixtures are shown.

One trend visible in all plots is that the DoS becomes noisier, when the mole fraction of the corresponding component is smaller. The DoS is averaged over all molecules of one type, therefore less of a component means worse statistics for the DoS.

The translational DoS of methanol and ethanol have, in contrast to water, only one large peak at low frequencies at around $20\,\mathrm{cm^{-1}}$ as seen in Figures 4.3c and 4.3g. Because it is the only visible peak, it is most likely caused from the direct oscillation of two molecules against each other in their LJ-potentials. The peak is blue-shifted by the addition of water. This results in a loss of entropy, because higher frequency oscillations have a smaller amplitude and therefore a lower entropy. The diffusion constant, which is proportional to the zero frequency value of the translational DoS, generally decreases by mixing. This effect is most strongly visible in the translational DoS of methanol in Figure 4.3c, where the zero frequency value is halved by the addition 60 % water. The effect of methanol on the diffusivity of water, shown in Figure 4.3a, is however very small. In the 2PT model the amount of

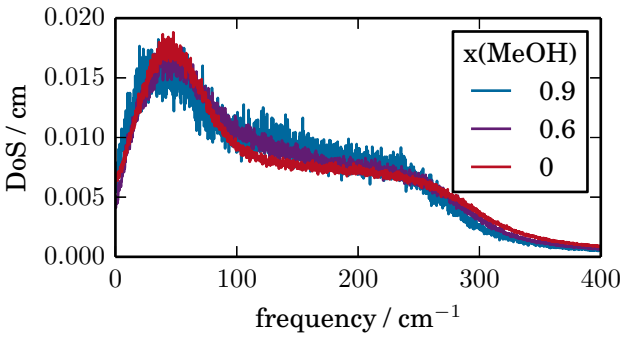

(a) Water translational DoS depending on x(MeOH).

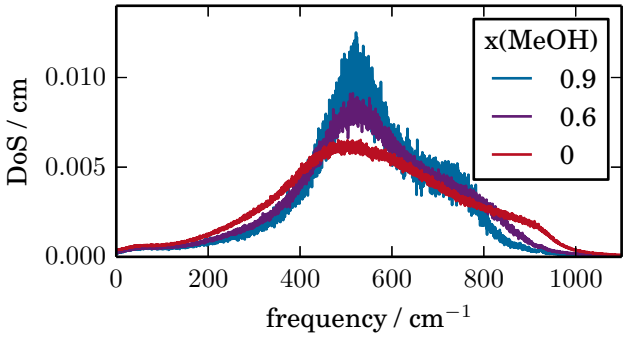

(b) Water rotational DoS depending on x(MeOH).

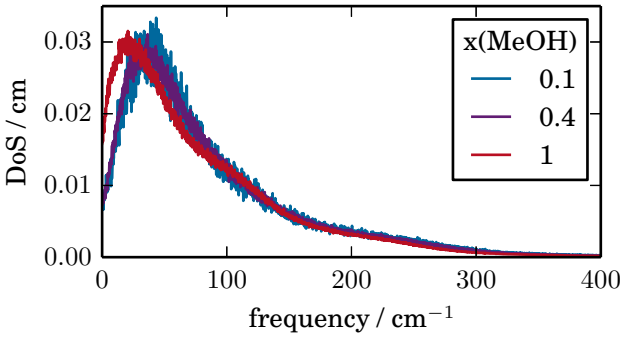

(c) Methanol translational DoS depending on x(MeOH).

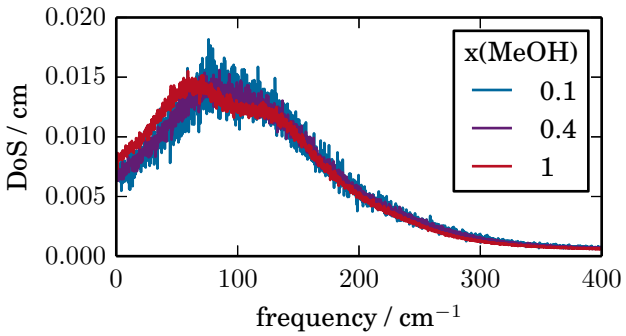

(d) Methanol rotational DoS depending on x(MeOH).

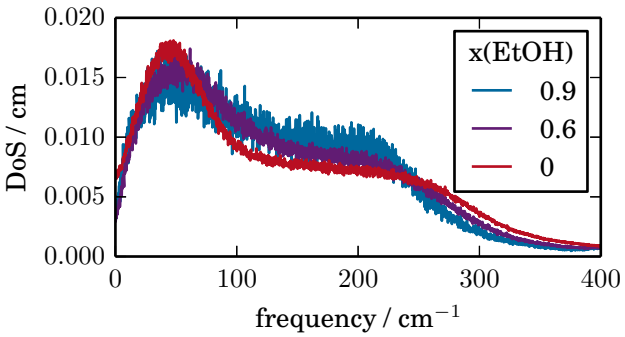

(e) Water translational DoS depending on x(EtOH).

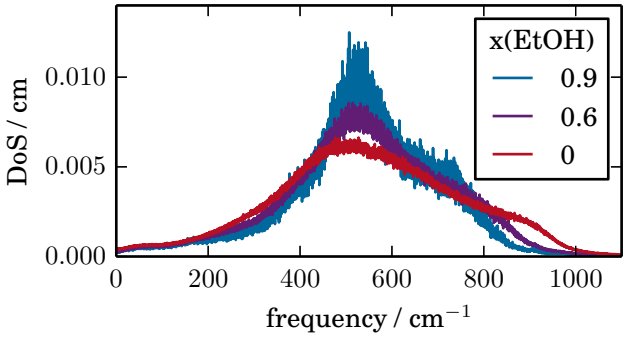

(f) Water rotational DoS depending on x(EtOH).

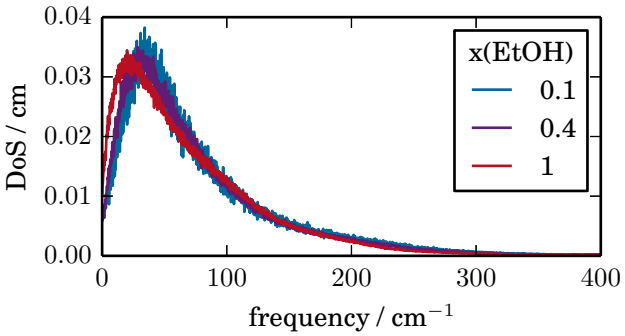

(g) Ethanol translational DoS depending on x(EtOH).

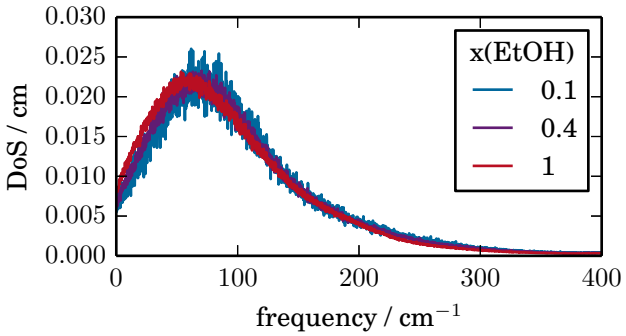

(h) Ethanol rotational DoS depending on x(EtOH).

Figure 4.3: The translational and rotational DoS of water, methanol and ethanol in water-methanol and water-ethanol mixtures. The red line is always the DoS of the component in the pure fluid. The changes due to mixing are manifold. A general trend is the lowering of the zero-frequency value of the translational and rotational DoS by mixing. This effect is strong for methanol when adding water, but weak for water when adding methanol. The alcohols change the dominant peak in the rotational DoS of water to become sharper. The peak in the translational DoS of the alcohols is blueshifted when adding water.

hard sphere gas is calculated from the zero frequency value. The gas has a high entropy, therefore a lower diffusion constant is connected to a loss of entropy.

The effects of methanol and ethanol on the rotational DoS of water (Figures 4.3b and 4.3f) are almost identical. The middle peak at 550 cm^{-1} becomes more defined, which is an interesting effect of the alcohol on the water. It is partially caused by the redshift of the highest frequency peak visible as a shoulder at around 900 cm^{-1} in the spectrum of pure water. That peak is related to the principal axis with the lowest moment of inertia. The corresponding libration has a lower frequency in alcohols. As these are changes at relatively high frequencies, they do not have a large influence on the rotational entropy.

All rotational densities of states have their zero frequency value lowered by mixing, showing that it is more difficult for molecules to reorientate in a mixture than in a pure liquid. This could be explained by the generally higher packing of the molecules in a mixture. By filling the holes with the smaller molecules the system becomes more dense, which is a well known behavior of water-alcohol mixtures. The side effect is that each molecule has less space to rotate.

This explanation can also be used for the decrease of the diffusion coefficients. In a more dense fluid the mean free path can be expected to be shorter, leading to a lowered diffusion.

4.2.2 Thermodynamics

The densities of states have been separated and weighted with the 2PT model to give the entropy of the mixture. These are compared to the ideal mixing entropy to give the excess mixing entropy

$$\Delta S^{\mathrm{E}} = S^{\mathrm{mix}} - S^{\mathrm{id.\ mix}} \tag{4.2}$$

$$S^{\mathrm{id.\ mix}} = \sum_h \left(x_h \, S_h^{\mathrm{pure}} - k x_h \ln x_h \right). \tag{4.3}$$

Here h is the component, so either methanol, ethanol or water and S_h^{pure} is the entropy of this component in its pure fluid. The resulting excess mixing entropies are shown in Figure 4.4 along with experimental minima.

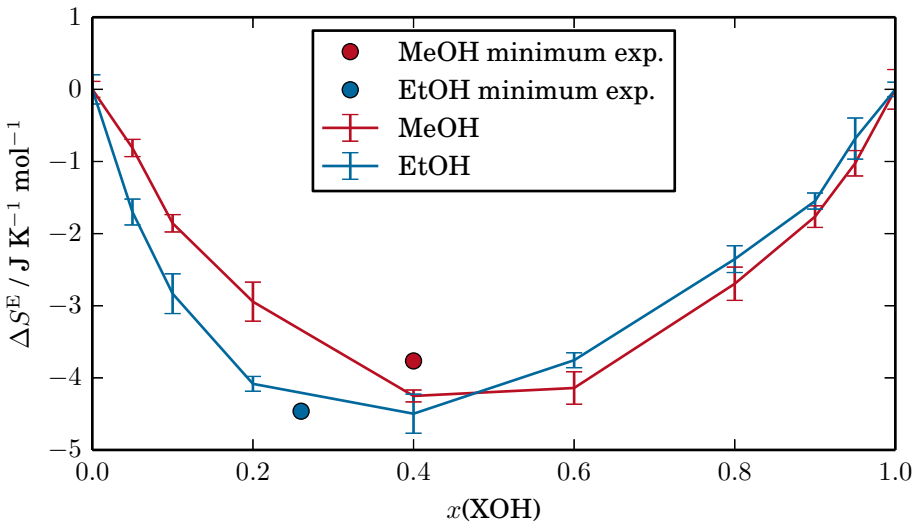

Figure 4.4: Excess mixing entropies of water-methanol and water-ethanol mixtures and experimental minima[20]. Both curves have a parabolic shape with the minimum at a mole fraction of 0.4 with a maximum entropy loss of 4.2 $\mathrm{J\,mol^{-1}\,K^{-1}}$ to 4.5 $\mathrm{J\,mol^{-1}\,K^{-1}}$. The correlation with the experimental values is reasonable.

The results conform reasonably with the depth of the experimental minima and well with their positions. This shows that the 2PT model is generally suited to predict mixing entropies very cheaply in terms of computational effort. Additionally it can be used to investigate the contributions to the entropy. The first step is to take a look at the contributions of each component. The excess entropy of a component is its entropy in the mixture minus its entropy in its own pure fluid

$$\Delta S_h^{\mathrm{E}} = S_h^{\mathrm{mix}} - S_h^{\mathrm{pure}}. \tag{4.4}$$

In Figure 4.5 the excess mixing entropy of a water-methanol mixture is shown with the contributions of the different molecules along with literature data from a previous study.

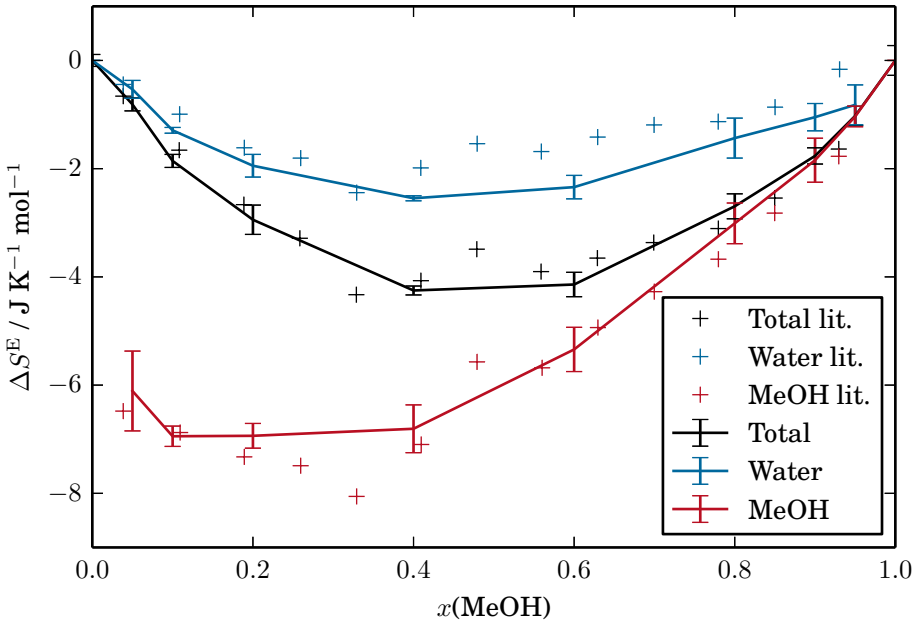

Figure 4.5: Excess entropy of a water-methanol mixture and the contributions from both components in comparison with literature data[12]. Water loses at most $2.5\,\mathrm{J\,mol^{-1}\,K^{-1}}$ of entropy in the mixture. Methanol loses up to $7\,\mathrm{J\,mol^{-1}\,K^{-1}}$. At high mole fractions of methanol the excess entropy of water approaches zero, implying that water has the same entropy in water as in almost pure methanol. The literature values are well reproduced.

The analysis of this system has been performed before[12] and the results are also plotted showing good conformance with the calculated values. The most important conclusion from the components contributions is that methanol loses far more entropy than water in the mixture, clearly visible in Figure 4.5. Interestingly Methanol loses about $6\,\mathrm{J\,K^{-1}\,mol^{-1}}$ of entropy at low concentrations in water, whereas small amounts of water in methanol have almost the same entropy as pure water.

The results for water-ethanol mixtures are shown in Figure 4.6. Here the picture is very different. Ethanol and water both contribute noticeably to the entropy loss. Water does lose about $4\,\mathrm{J\,K^{-1}\,mol^{-1}}$ of entropy when mixed in ethanol, in contrast to water in methanol. This could be the result of ethanol being more hydrophobic. I expect the entropy loss to be even higher for propanol and higher alcohols, leading to a higher chemical potential of water in those mixtures and at some point to immiscibility. Ethanol loses entropy in mixtures with high water content (about $4\,\mathrm{J\,K^{-1}\,mol^{-1}}$).

Each of the components contributions can be further split up into the translational and rotational contribution they were calculated from. The graphs are shown in Figure 4.7. The entropy loss is mainly caused by the translational motion in all cases. The rotational entropy of each component is lowered by about $1\,\mathrm{J\,K^{-1}\,mol^{-1}}$ by mixing.

On this level we can now understand, why water in methanol has only a small entropy loss. Figure 4.7b shows that the water molecules translational entropy instantly decreases for low mole fractions of methanol whereas it increases at high mole fractions until it cancels out the entropy loss from the rotation. With ethanol in Figure 4.7d the translational entropy loss also decreases at high mole fractions of ethanol, but it never results in an entropy increase. Therefore water is entropically more favored in methanol than in ethanol.

The results do not support the entropy loss by molecular segregation, neither for methanol nor for ethanol. In both cases the entropy loss of the alcohol is present at low mole fractions. With only few alcohol molecules present the formation of clusters or chains is unlikely and has not been observed in the molecular dynamics trajectory. So at least for those concentrations the negative excess entropy can not be explained by molecular segregation.

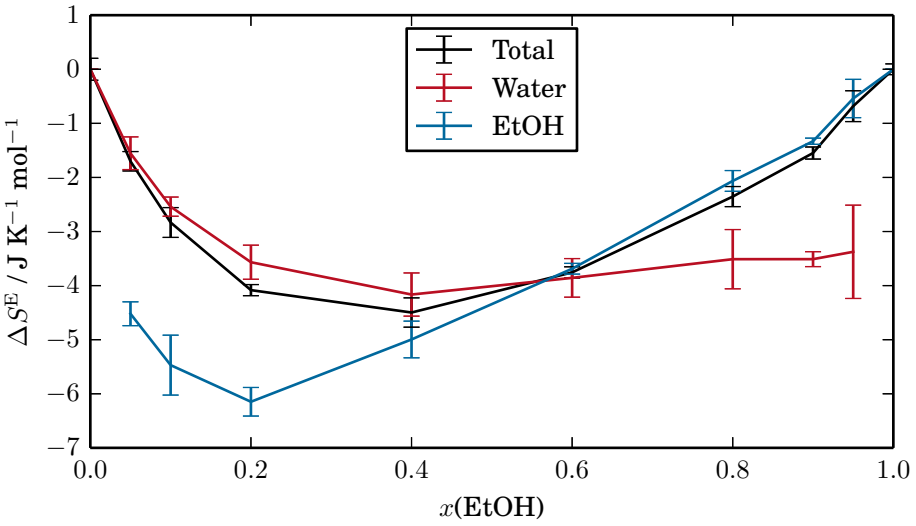

Figure 4.6: Excess entropy of a water-ethanol mixture and the contributions from both molecules. Ethanol has a maximal entropy loss of $6\,\mathrm{J\,mol^{-1}\,K^{-1}}$ at a mole fraction of 0.2. Water does contribute to the total entropy loss with $4\,\mathrm{J\,mol^{-1}\,K^{-1}}$ at most mole fractions.

The translational entropy is calculated as a sum of a diffusive and an oscillating subsystem. In Figure 4.8 the entropy loss of methanol is shown again, this time with the translational contribution split up into the diffusive and oscillating parts.

In comparison with the reference plot also shown in Figure 4.8 a mismatch is visible. The diffusive and oscillating (red and blue, respectively) curves do in either case add up to the translational curve (green), but each one deviates from literature. This indicates, that I made a deviating separation in hard sphere gas and oscillators. This is expected, because I did not implement the correction made to the compressibility (see Section 2.2.5). It is quite surprising, that with a different separation scheme, the total entropy of the hard sphere gas and the harmonic oscillators matches the literature results. The 2PT model seems to be very stable to fluctuations in the fluidicity factor. This may indicate a cancellation of errors. But more importantly it shows that the division into a hard sphere gas and harmonic oscillators should not be interpreted physically.

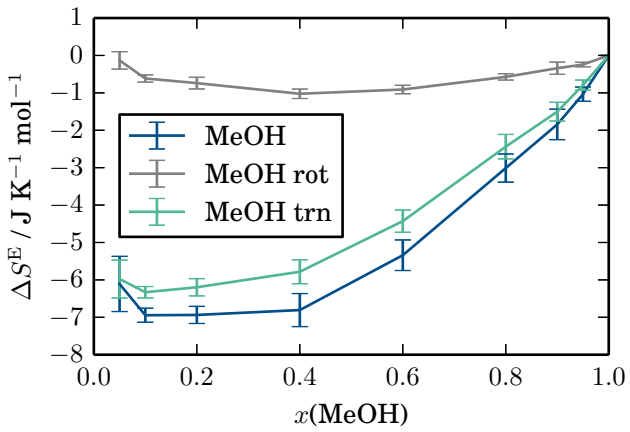

(a) Excess entropy of methanol in a water-methanol mixture.

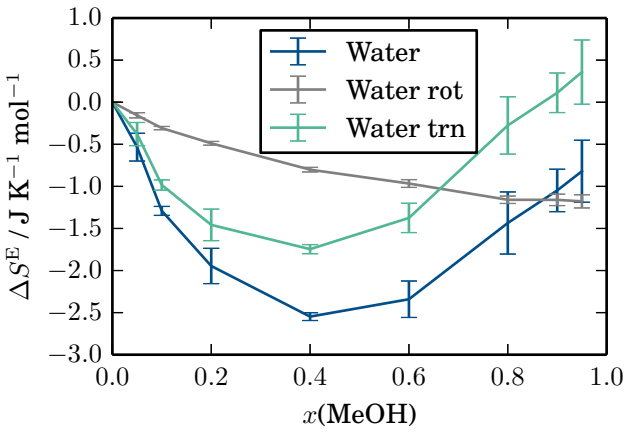

(b) Excess entropy of water in a water-methanol mixture.

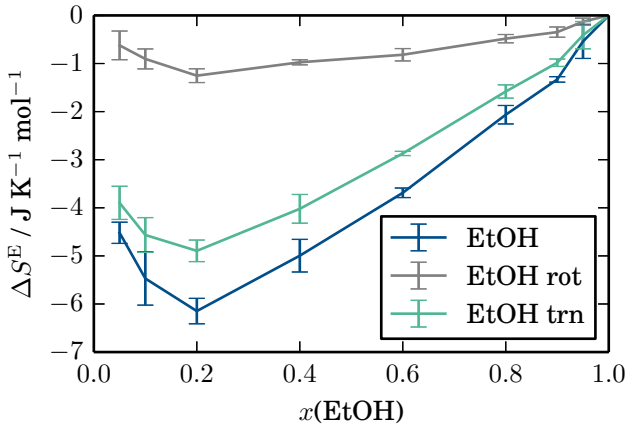

(c) Excess entropy of ethanol in an water-ethanol mixture.

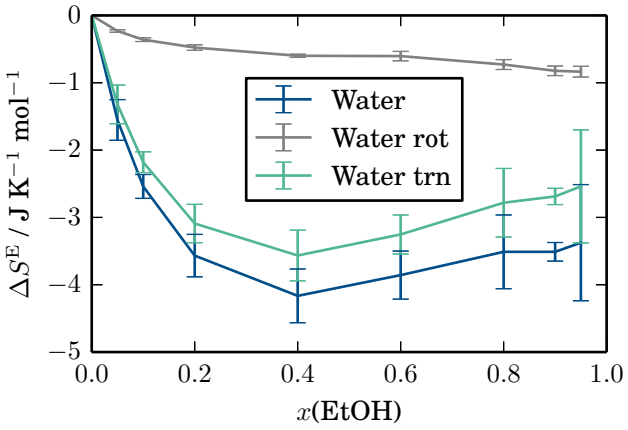

(d) Excess entropy of water in an water-ethanol mixture.

Figure 4.7: The contributions to the excess mixing entropy of methanol water and ethanol water. In every case the rotational contribution is around $-1\,\mathrm{J\,mol^{-1}\,K^{-1}}$. The translational contribution is in most cases dominantly responsible for the entropy loss. Only for the case of high mole fractions of methanol the translational contribution is positive.

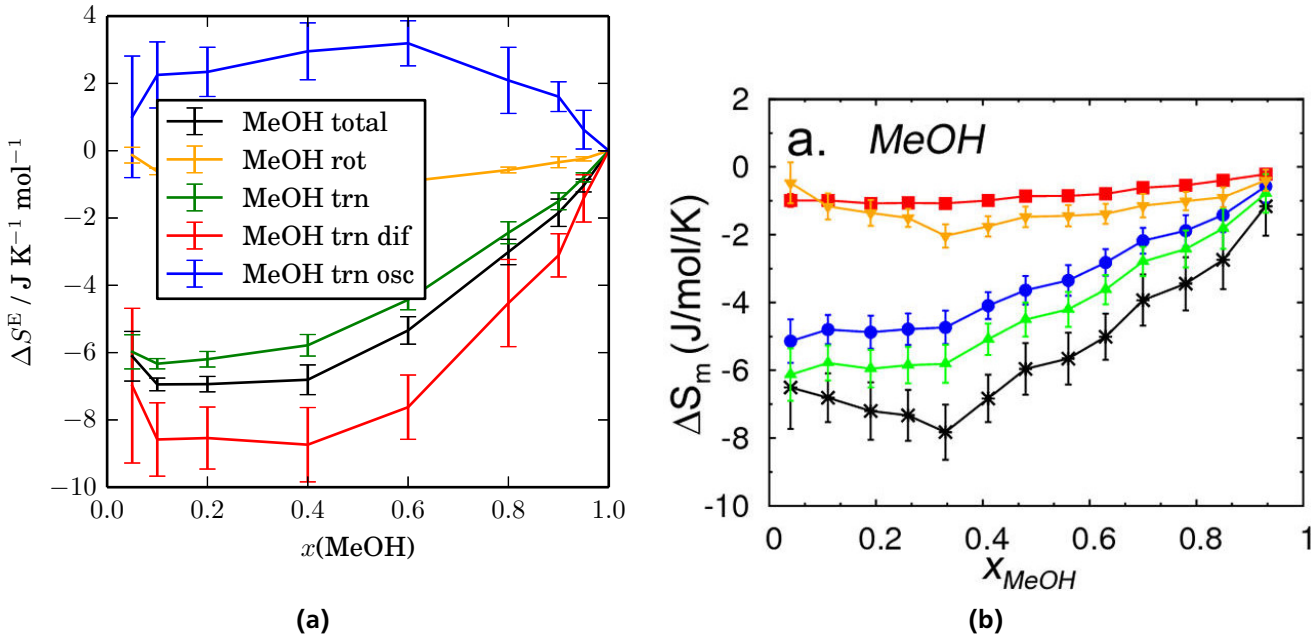

(a) (b)

Figure 4.8: Excess entropy of methanol in water. The translational contribution was further broken down into the diffusive and the oscillating contribution. (a) are the results of this work and (b) is taken from literature[12]. The translational and rotational contributions do correlate with the reference data. The separation of the translational contribution into diffusive and oscillating is very different from the literature.

4.3 Sodium Chloride Solutions

Sodium chloride is chosen as an example system to test the influence of ions on the water dynamics and thermodynamics.

Systems with 0, 50, 100, 200, 300, 400, 500 and 1000 sodium and chloride ions with the 10000 water molecules have been analyzed. For the system with 1000 NaCl partial crystallization was observed during the molecular dynamics simulation.

4.3.1 Dynamics

The densities of states of the components are shown in Figure 4.9. The ions have no rotational DoS because they are spherical particles. All densities of states show the hydrogen bond bending peak at 50 cm^{-1}. Na^+ has two additional peaks which can not be assigned directly. Cl^- has only one additional peak, which makes its DoS look much like the one of water. The effect of the ions on the dynamics of water is only visible in the translational DoS. There the diffusion coefficient and the first peak decrease and the density is shifted to mid frequency regions at around 110 cm^{-1}.

The separated contributions also shown in Figure 4.9 change the view on the density shift slightly. The decrease of the first peak is due to the decrease of the hard sphere DoS, which is superpositioned with the oscillating DoS. This indicates, that the hydrogen bond bending is not affected by NaCl, only the diffusion coefficient and some mid-frequency oscillation. However, studies find that the number of hydrogen-bonds in general is decreased by NaCl[39]. As we will see in Section 5.2, the superposition of the diffusive and oscillating DoS is not necessarily right. Therefore the picture the 2PT model gives is to be doubted and the decrease of the first peak is likely not purely an effect of lower diffusion.

The diffusional DoS of water at different salt concentrations all show the same behavior, only with varying starting points. The diffusional DoS of the ions however do show very different behavior depending on the salt concentration. The decay has different widths. This seems to be an effect of the separation, and it is unclear whether it refers to an actual physical effect or shows a problem of the empirical formulas used for the separation.

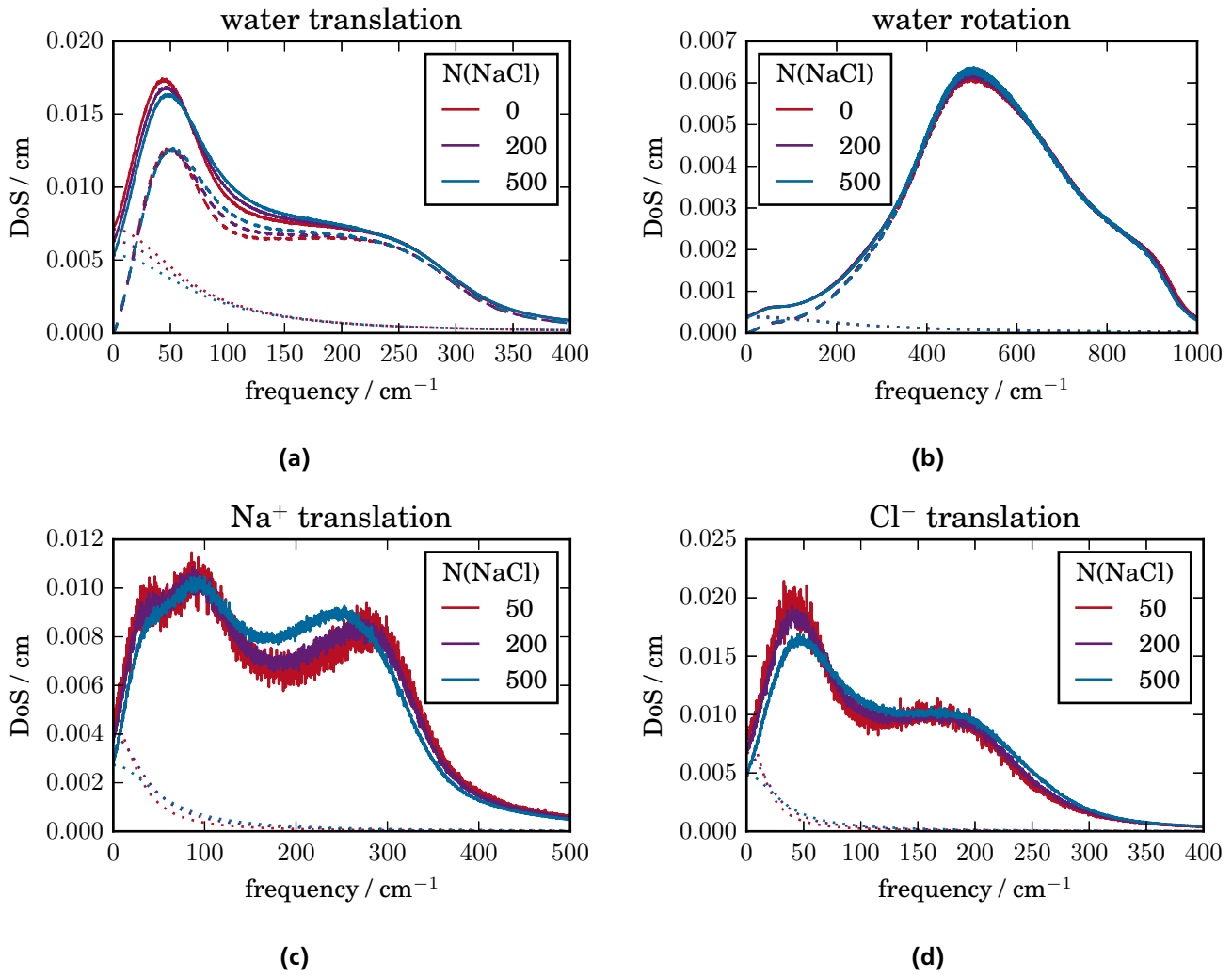

Figure 4.9: The densities of states of water, Na^+ and Cl^-. Additionally the diffusive (dotted) and oscillating (dashed) contributions are displayed. For the ions the oscillating DoS is left out for clearance. The sodium DoS has three visible peaks, while the chloride DoS looks much like the one of water. All translational densities of states show a decrease of the diffusion coefficient with higher salt concentrations. For water that energy density is shifted to oscillating modes with a frequency of $110\,\mathrm{cm}^{-1}$.

4.3.2 Thermodynamics

For solutions of ions no excess mixing entropy can be calculated, because there is no accessible reference state for the ions. We can however calculate the (molar) entropies of water and the ions and analyze their dependence on the salt concentration, which are shown in Figure 4.10.

The molar entropy of water decreases with increasing salt concentration almost linearly. The reason for this decrease is the lower diffusion coefficient, as shown in the last section. The molar entropy of the chloride ion also decreases with increasing concentration. The slope is steeper for chloride. Na^+ shows an interesting behavior. Its molar entropy increases upon addition of salt to have a maximum at circa $1\,\mathrm{mol\,l}^{-1}$ and then decreases. This can be explained from two different density shifts visible in the DoS of Na^+ in Figure 4.9d. One is the redshift of the peak at $300\,\mathrm{cm}^{-1}$ with growing salt concentration, which causes an entropy gain. The other is the loss of diffusional entropy by a decreasing zero frequency value.

The entropies calculated for this system have not been compared to experimental values yet, because they are not easily obtained experimentally. The problem is the choice of the reference system. It is possible to calculate the mixing entropy with the ions being an ideal gas for example. But this is not a value that can be referred to an

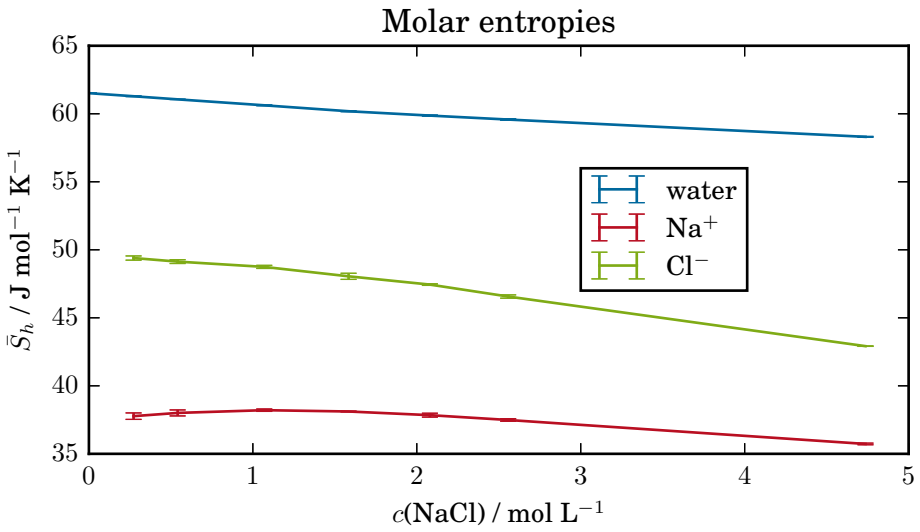

Figure 4.10: The molar entropies of water, Na^+ and Cl^- in dependence of the salt concentration. For water and the sodium ion the molar entropy is decreasing with increasing salt concentration. The molar entropy of the chloride ion has a maximum at a concentration of $1\,\mathrm{mol\,l^{-1}}$.

experiment. Also experiments usually report the free energy difference, but with the solvation of ions the energetic contribution is usually dominant.

One possibility to make comparison to experiments would be the calculation of the chemical potential of water. For this the molar enthalpy of water would be needed, in addition to the molar entropy. Generally it should be possible to calculate the molar enthalpy from a MD simulation. The chemical potential can be compared with osmosis or partial pressure experiments.

5 Advancing 2PT Model

A big problem of the 2PT model is the use of hard sphere theory. As shown it should not be used for the separation of the rotational DoS. But even for the translational degrees of freedom it is questionable if the results are always reasonable, because the Carnahan-Starling equation of state is empirical. It also remains unclear what this separation means on a microscopic level. The thermodynamic properties are calculated as if the system consisted of two noninteracting subsystems, a set of harmonic oscillators and a hard sphere gas. But obviously all atoms/molecules have the same intermediate motion. Every translational and rotational degree of freedom is to some part diffusive and oscillating. Here I report three different approaches, that aim to perform the separation within a microscopic model.

5.1 Time Separation

The 2PT model suggests, that the diffusional motion has only kinetic energy, while the oscillating motion has both kinetic and potential energy for each DoF. One way to interpret this on a microscopic level is that the particle's motion is divided into short time spans, where the particle moves freely (with constant velocity) and others, where it is trapped in a harmonic potential of some frequency. A sketch is given in Figure 5.1.

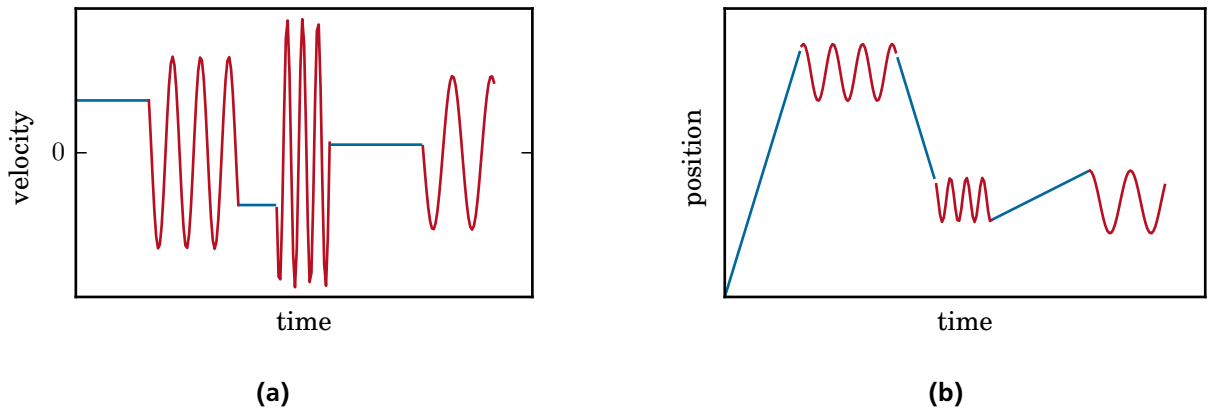

Figure 5.1: The velocity (a) and position (b) development for a simple model, that describes the diffusive motion through short constant velocity flights and the oscillation as short time spans in which the particle's movement is equal to that of a harmonic oscillator. The length of all spans can vary. The oscillation's frequencies and the free flights velocities are distributed.

Obviously these graphs do not have a lot in common with molecular dynamics trajectories, but they reassemble the needed properties. The free flight time spans with different velocities and length and lead to a random motion which explains why there is diffusion. The time spans where the motion is trapped in harmonic potentials with different frequencies account for the oscillating part of the density of states. The fluidicity factor f is the fraction of time, in which the DoF is not trapped in a potential.

Since the actual trajectory looks very different, there is no way to identify these time spans. There is a property that could allow separation: the absolute of the rate at which potential and kinetic energy are exchanged, P. In the model above during the free flight time spans this energy exchange is zero. During the harmonic oscillation this energy exchange it is equal to the value expected from a harmonic oscillator with the same frequency, which is

$$P(\nu) =< |P_{\mathrm{HO}}(\nu)| >= 4E_{\mathrm{tot}}\,\nu = 4kT\,\nu. \tag{5.1}$$

A harmonic oscillator exchanges its total energy four times during on period of $T = 1/\nu$. By integrating this measure over the DoS all degrees of freedom are treated as harmonic oscillators

$$P_{\mathrm{DoS}} = \int_0^\infty S(\nu)P(\nu)\,\mathrm{d}\nu \tag{5.2}$$

It is also possible to obtain P from a trajectory, because the power of exchange from potential to kinetic energy is equal to velocity times force

$$P_{\text{Traj}} =< |v \cdot P| > . \tag{5.3}$$

P_{DoS} and P_{Traj} should be equal for systems which are purely oscillating. When part of the DoS is from free flight, P_{DoS} should be larger than P_{Traj}.

This was tested on four systems: A set of 300 independent harmonic oscillators at constant temperature and a system of 500 LJ atoms at solid ($T^* = 1.1, \rho^* = 1.1$, ffc crystal), liquid ($T^* =, \rho^* = 1.1$) and gaseous phase ($T^* =, \rho^* = 1.1$). The densities of states are shown in figure 5.2. The DoS of the harmonic oscillators shows as expected a single peak. The LJ solid has a distribution of peaks without a zero-frequency value. The LJ fluid and gas both have a zero-frequency value indicating diffusion, but only the fluid shows a local maximum, while the DoS of the gas decays monotonically.

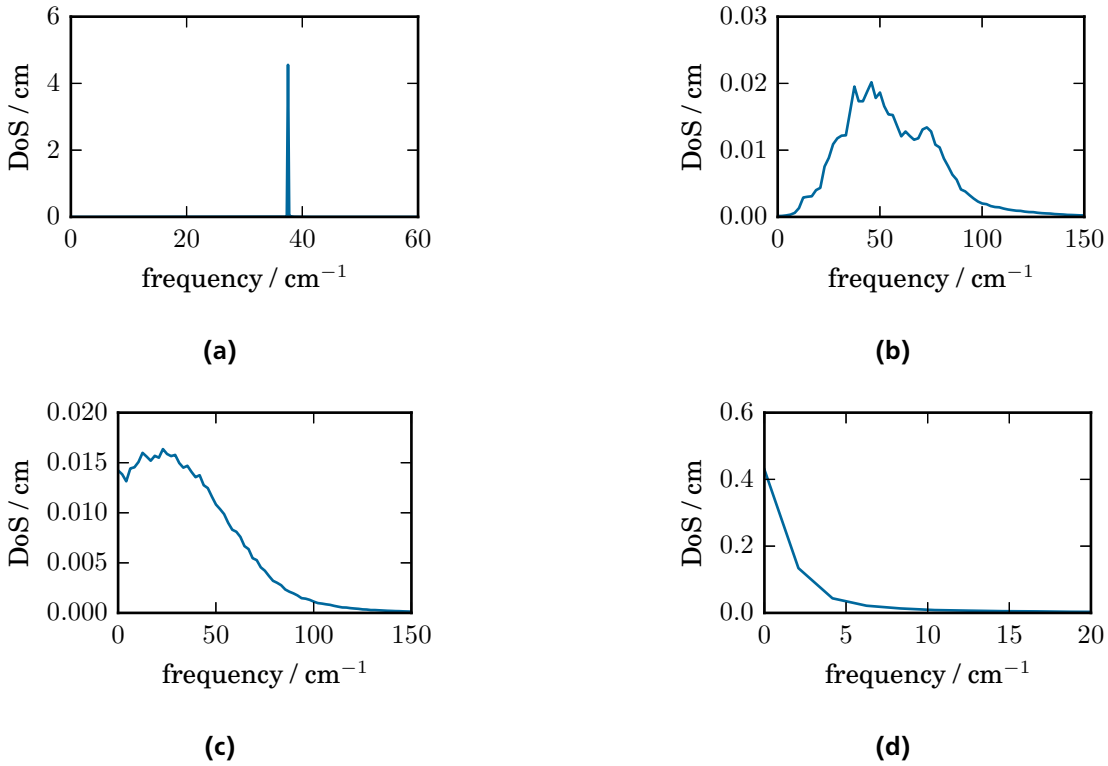

Figure 5.2: Densities of states of (a) a set of harmonic oscillators, (b) LJ solid, (c) LJ liquid and (d) LJ gas. The DoS of the harmonic oscillators is a single peak, the DoS of the solid shows a distribution of oscillations. The DoS of the liquid has a zero-frequency value, increases to a maximum and then decreases. The DoS of the gas is monotonically decreasing.

Table 5.1: Absolute of energy exchange from the trajectory and from treating the whole DoS as harmonic oscillators.

	P_{Traj} / kJ mol^{-1} ps^{-1}	P_{DoS} / kJ mol^{-1} ps^{-1}
HO	3.672	3.676
LJ crystal	7.746	7.493
LJ fluid	5.358	4.939
LJ gas	0.5860	0.6613

The results are shown in Table 5.1. The harmonic oscillators give the same rate of energy exchange by integrating over the density of states and from the trajectory. The LJ crystal has a higher P_{Traj} than P_{DoS}. Since there is no diffusion and all motions are oscillating the deviation has to be a result of anharmonic oscillations. For the fluid

the results are similar to the solid, even though one could expect that P_{DoS} would be larger as it treats the diffusive part in the DoS as harmonic oscillations. In the gaseous system this is finally the case, but the values are still close. This is surprising, because for a dilute system one could expect that the atoms are moving freely most of the time and P_{Traj} is significantly lower.

From these observations it becomes clear, that the exchange of energy is not a good measurement of the diffusivity of a system. But even though these results do not lead to a new method for separating the DoS, there are two interesting aspects to it. First, the results for the crystal showed that even though all motions are oscillating, they do not seem to be fully harmonic. Second, in a gas of LJ particles the atoms are not moving as freely as one expects from the DoS.

5.2 Velocity Separation

From the attempt in the last section we learned, that even a LJ gas, which is highly diffusive, is exchanging a large degree of kinetic and potential energy. This observation leads to my second attempt to explain the 2PT model on a microscopical level, which allows each particle to be oscillating *during* the diffusion.

The idea is to describe the velocity as a sum of two components, one that accounts for the diffusion and one for the oscillation

$$v = v^{\mathrm{dif}} + v^{\mathrm{osc}}. \tag{5.4}$$

The trajectory of each DoF is divided into pieces at the local extrema of the velocity. For each piece the mean is calculated and the consecutive of all constant pieces is the diffusive part v^{dif}. The oscillating part v^{osc} is the trajectory's velocity, minus the diffusive part. Since the total velocity and the diffusive velocity have the same mean for each piece, the oscillating part has a zero mean. The DoS calculated from v^{osc} has therefore no zero frequency value. A sketch is given in Figure 5.3.

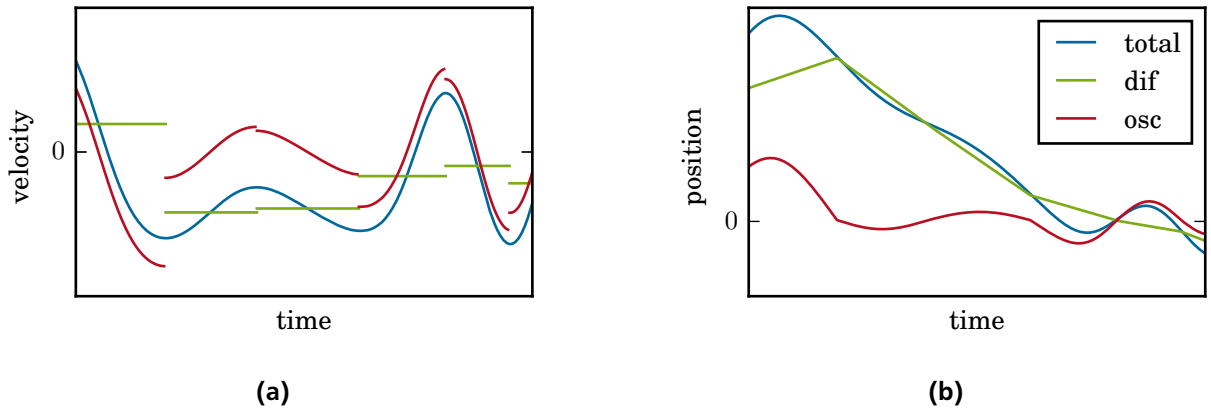

Figure 5.3: The velocity (a) and position (b) of simulated LJ system is shown in blue. For every piece between two extrema the mean of the velocity is subtracted from the velocity, which results in the red pieces that have zero mean. This is the oscillating part. The diffusive part consists of the green constant functions, that contain the mean of the velocity between the two extrema. This is the diffusive part of the model. The positional curves are obtained by integrating the velocity.

The decision to make the cuts at the turning points of the velocity is what defines this idea and has to be questioned, because it can seem very arbitrary at first. The idea behind it is that an atom (or rather one of its DoF) moves to a different surrounding every time it is moving fast in one or the other direction. It is at a local minimum along its path on the potential energy surface and the shape of the potential is assumed to be different on the other side.

A different way to put it, is the assumption that there are no superpositions of oscillations, because the surrounding of an atom changes randomly on the same time scale on which it performs its oscillations. From that one can already see cases, where this model will break down. In crystals there are lattice vibrations, which have significantly lower frequencies. In that case superposition of oscillations plays an important role. But also in a fluid, if there are atoms with a large difference in their mass the translational movement of the lighter atom could to some extend be a superposition of its own oscillation and the oscillation of the heavier atom.

From the separated velocities, the densities of states can be calculated the usual way similar to Equation (2.1) (in this section i use $\mathscr{F}$ for the Fourier transform, for convenience)

$$S^{\mathrm{dif}}(\nu) = \frac{2m}{kTN} \sum_{i=1}^{N} \sum_{k=1}^{3} \left| \left(\mathscr{F} v_{i,k}^{\mathrm{dif}} \right)(\nu) \right|^2 \tag{5.5}$$

$$S^{\mathrm{osc}}(\nu) = \frac{2m}{kTN} \sum_{i=1}^{N} \sum_{k=1}^{3} \left| \left(\mathscr{F} v_{i,k}^{\mathrm{osc}} \right)(\nu) \right|^2 . \tag{5.6}$$

The diffusive and the oscillating DoS do not add up to the total DoS as in the 2PT model

$$S(\nu) = \frac{2m}{kTN} \sum_{i=1}^{N} \sum_{k=1}^{3} \left| \left(\mathscr{F}(v_{i,k}^{\mathrm{dif}} + v_{i,k}^{\mathrm{osc}}) \right)(\nu) \right|^2 \tag{5.7a}$$

$$= \frac{2m}{kTN} \sum_{i=1}^{N} \sum_{k=1}^{3} \left| \left(\mathscr{F} v_{i,k}^{\mathrm{dif}} \right)(\nu) + \left(\mathscr{F} v_{i,k}^{\mathrm{osc}} \right)(\nu) \right|^2 \tag{5.7b}$$

$$= \frac{2m}{kTN} \sum_{i=1}^{N} \sum_{k=1}^{3} \left| \left(\mathscr{F} v_{i,k}^{\mathrm{dif}} \right)^2(\nu) + \left(\mathscr{F} v_{i,k}^{\mathrm{osc}} \right)^2(\nu) + \left(\mathscr{F} v_{i,k}^{\mathrm{dif}} \right)(\nu) \cdot \left(\mathscr{F} v_{i,k}^{\mathrm{osc}} \right)(\nu) \right| \tag{5.7c}$$

$$\neq S^{\mathrm{dif}}(\nu) + S^{\mathrm{osc}}(\nu) \tag{5.7d}$$

This is an interesting result, because it questions the basic idea of the 2PT model, that a density of states can be described as an addition of two contributions directly in frequency space.

The results show, that the sum of the integrals of $S^{\mathrm{dif}}(\nu)$ and $S^{\mathrm{osc}}(\nu)$ equals the integral of $S(\nu)$. This reflects, that by splitting the velocity in two parts, the kinetic energy is also split. This separation scheme was tested with the same four systems, that were investigated in the last section. The resulting densities of states are shown in Figure 5.4.

For the set of harmonic oscillators both methods give the same separation. The peak is a bit lower with velocity separation, which could be a convergence problem. The solid system's density of states in Figure 5.4b is separated incorrectly. The oscillations with low frequencies are identified as diffusive states. This breakdown was partially expected, because as written before in solids there are lattice vibrations, which superpose the atom's vibration. By slicing the velocity at every extremum the superposition of low frequency oscillations is neglected. The 2PT model gets this right. For the LJ liquid and gas the results are in good agreement with the 2PT model. In Figure 5.4c it becomes apparent, that $S^{\mathrm{dif}}(\nu)$ and $S^{\mathrm{osc}}(\nu)$ do not add up to the total DoS as they do in the 2PT model.

The most interesting aspect of this proposed scheme is that it can be used to separate the rotational DoS in the same fashion. That would solve the big problem 2PT model has, as shown in Section 2.3.5. Only for demonstration and without calculating any properties from it the separation scheme is applied on the trajectory of the same system from Figure 2.3b. Contrary to the original decomposition scheme, it decomposes the rotational DoS nicely as can be seen in Figure 5.5.

For liquid water the results become more complex again. The decomposition predicted from velocity separation is given in Figure 5.6.

The diffusive part of the DoS is clearly not purely diffusive, but has a peak at $45\,\mathrm{cm}^{-1}$, which is a contribution from the hydrogen bond bending. The reason, why it has not been separated out is, the same as for the crystal: The oscillations are superpositioned and by cutting the velocity at every extrema, only the highest frequency oscillation is filtered out.

This is a major flaw of this decomposition scheme. It breaks down, as soon as there are two or more oscillations affecting the degrees of freedom simultaneously.

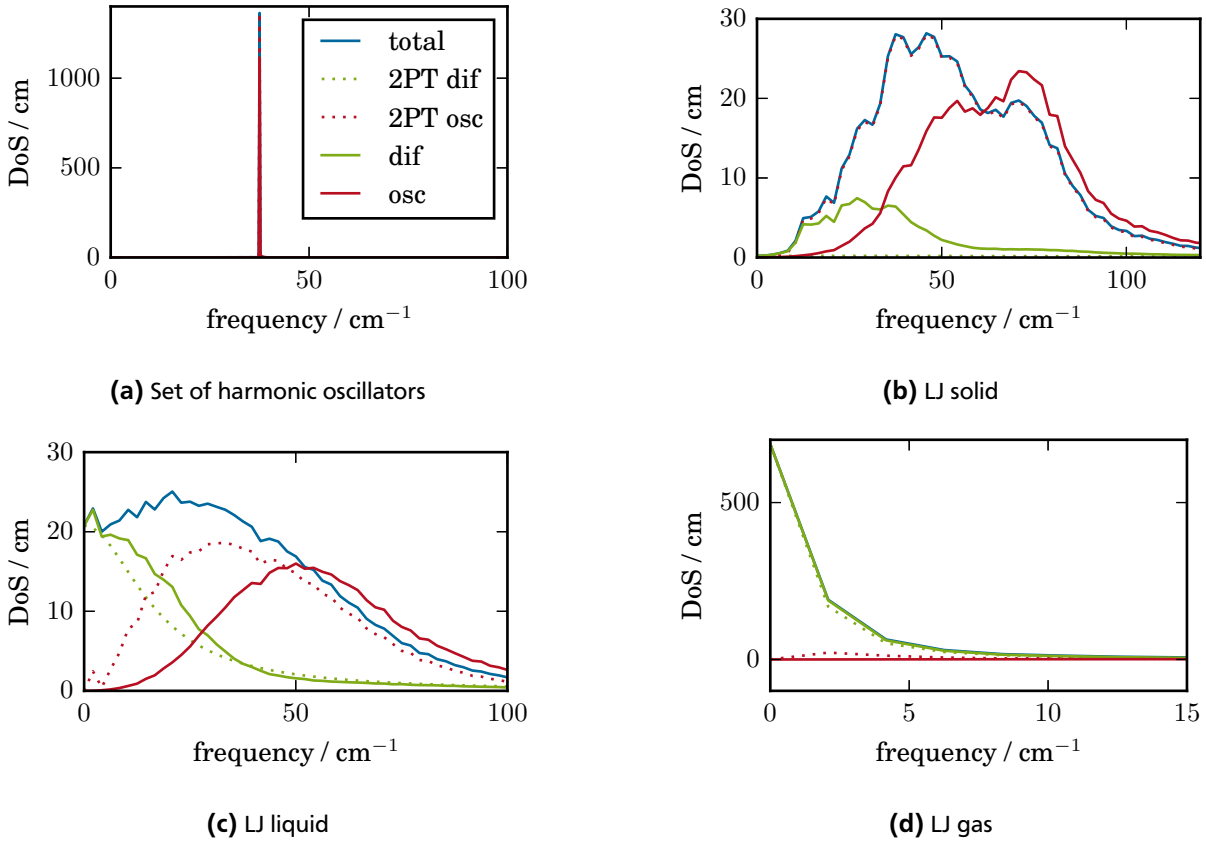

(a) Set of harmonic oscillators

(b) LJ solid

(c) LJ liquid

(d) LJ gas

Figure 5.4: The translational DoS of four systems and their separation in diffusive and oscillating motions obtained by the 2PT model (dotted, green and red) and by slicing at velocity extrema (solid, green and red). The separations are identical for the harmonic oscillators and the LJ gas. For the LJ solid some part of the DoS is falsely identified as diffusive contribution. The DoS od the liquid is separated in a comparable way by both methods, but with the velocity separation the contributions do not add up to the total DoS.

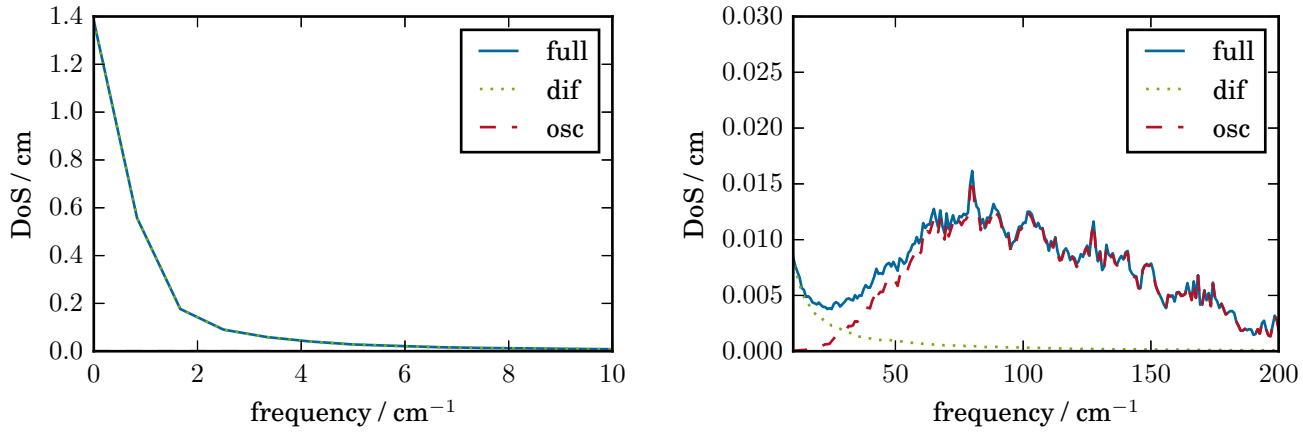

(a)

(b)

Figure 5.5: The density of states of water vapor at 500 K and $\rho = 2.5\,\mathrm{kg\,m^{-3}}$ in two different frequency regimes. The DoS is correctly separated by the velocity separation scheme.

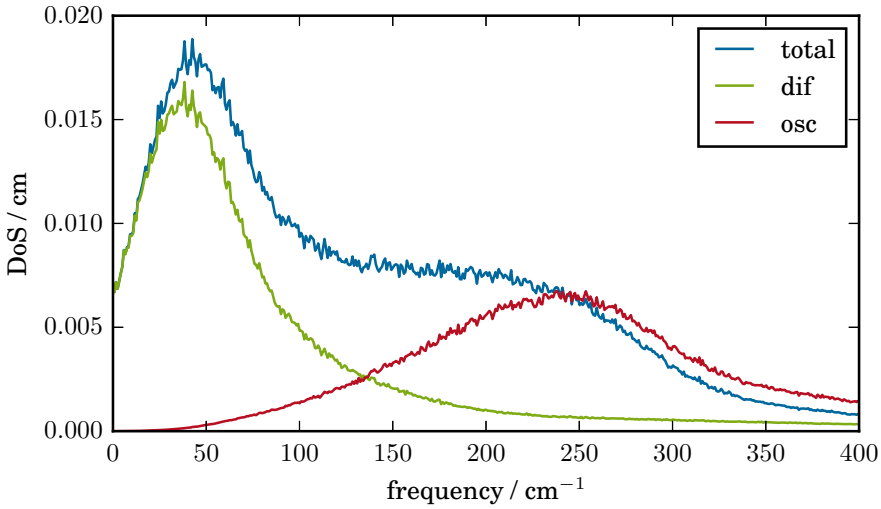

Figure 5.6: Translational density of states of liquid SPC/E water and its decomposition predicted by velocity decomposition. Only the highest frequency oscillation of water at 250 cm^{-1} is identified as an oscillating motion. The peak at 50 cm^{-1} is incorrectly identified as diffusive motion.

5.3 Position Separation

This scheme works very similar to the one of the last section. The separation is made on the positional trajectory

$$r = r^{\mathrm{dif}} + r^{\mathrm{osc}}. \tag{5.8}$$

On this level the separation can be understood most easily. The diffusive motion is a slow, uncorrelated movement through the volume of a system. The oscillating motion is a superposed vibration. The velocity is the derivative of the position, therefore this separation follows the same ansatz from the last section, only the separation is performed differently.

The idea is that by smoothing the positional development of a DoF one loses all oscillations and what remains is a diffusive motion. For the smoothing a Gaussian filter has been used. A decomposition of a positional trajectory of a water molecule is shown in Figure 5.7. The oscillating motion, which is again the total minus the diffusive motion, is not shown for clarity.

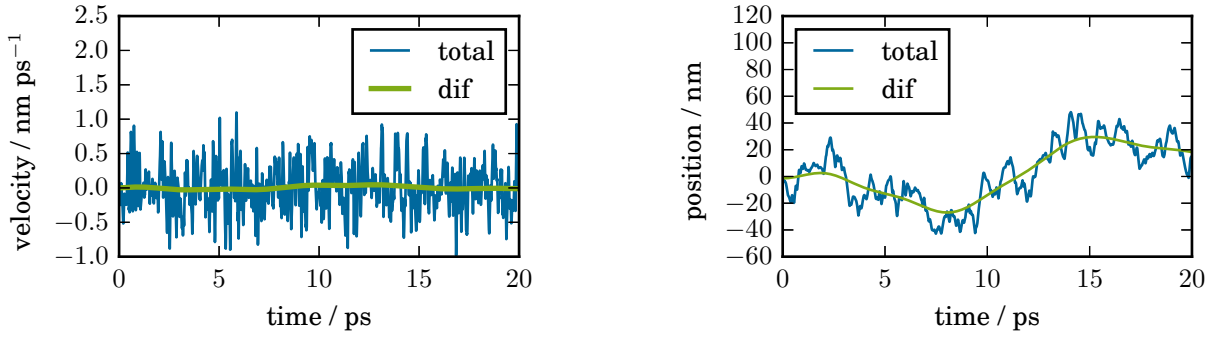

(a) **(b)**

Figure 5.7: The velocity (a) and position (b) of simulated SPC/E water molecule is shown in blue. The position trajectory has been smoothed out to give the diffusional contribution shown in green. The filter width was chosen such that the VAC function of the diffusional movement is monotonically decreasing.

The problem to be solved by this kind of decomposition is to choose the right width for the Gaussian filter in order to separate out all oscillations, but no “random”, diffusional motions. In the limit of a very small filter width

no oscillations are filtered out, because the diffusional positions then equal the original positions. With a very large filter width the whole trajectory is smoothed out to a slow movement from the start to the end point. In between there is a value, where the smoothed positional movement follows the trajectory but has a VAC function that is only decaying. This can be interpreted as a property of a random motion. So the criterion is to find the smallest filter width for which the VAC function is only decaying. This was done by hand for the diffusional motion shown in Figure 5.7, but it should be simple to achieve this by an algorithm. The value used in the end for filter width is 1.2 ps. The resulting VAC of the diffusive motion is shown in Figure 5.8.

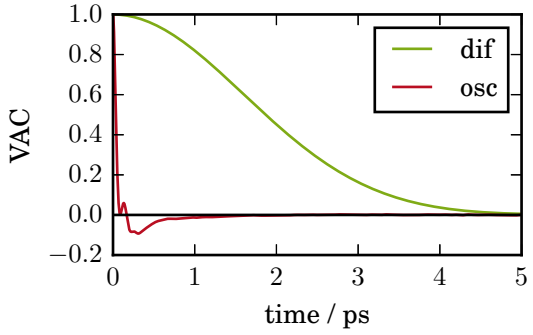

Figure 5.8: VAC function of the oscillating and the diffusive motion of liquid SPC/E water. The latter was obtained by smoothing the positions with a Gaussian filter.

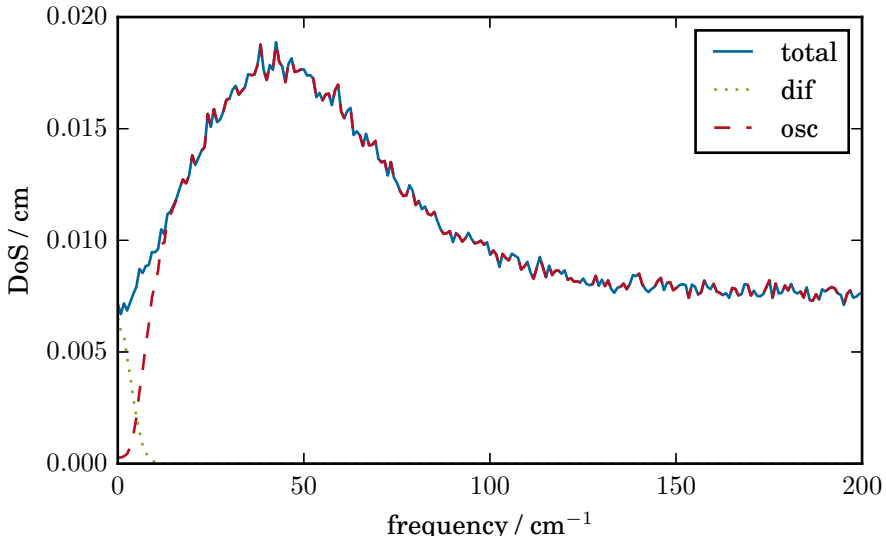

Figure 5.9: The translational density of states of liquid SPC/E water with the diffusional and rotational contribution separated by smoothing out the positions.

The translational DoS of liquid water with this separation carried out is shown in Figure 5.9. The oscillating DoS does not start exactly at zero, which is a boundary effect of my current implementation. The smoothed diffusive position does not start and end at the same value as the original position as an effect of the Gaussian filter. This should be easy to repair, but was not done yet.

Again we can observe that the total DoS is not equal to the sum of the two contributions, as was already explained in the last section. With this new separation scheme only a small part of the system is diffusive and the first peak is purely oscillating, which is not the case in the 2PT model.

The position separation scheme should work in this form also on rotational DoF and should be general. However, further investigations have to be performed in order to determine how meaningful and accurate this separation is.

5.4 Thermodynamic Properties

The velocity separation and position separation from Sections 5.2 and 5.3 split the motion of each particle into two parts, which changes the way the entropy is calculated from the resulting densities of states.

Every particle has a diffusive motion, but in this motion only a part of the kinetic energy is stored, the rest is in oscillations. This means that we can assign a temperature to the diffusive and oscillating motions. Their sum is the temperature in the system. The fluidicity factor would then be defined by

$$f = \frac{< v_{\mathrm{dif}}^2 >}{< v^2 >}. \tag{5.9}$$

This means that the thermodynamic properties should be calculated from two subsystems with the full number of particles but with **split temperature instead of with split particle number** and equal temperature as proposed by the 2PT model.

The diffusive subsystem now accounts for every particle slowly moving through the system with a “diffusion temperature”. The oscillating subsystem is the superposed fast motion of every particle. This gives a very physical picture of what the separation means on microscopical level.

There have been no entropies calculated with this method yet. But I would suggest making some tests by weighting the diffusive subsystem with the ideal gas entropy of N particles with a temperature of fT and the oscillating subsystem with the entropy of N classical harmonic oscillator with a spectral distribution of the energy according to the oscillating DoS and a temperature of $(1-f)N$.

This separation scheme also solves the inconsistency of the 2PT picture where only the diffusive fN particles are considered indistinguishable and the other $(1-f)N$ are distinguishable. In the new picture all N particles are indistinguishable, unaffected by how much kinetic energy is in a diffusive motion.

6 Conclusion

The Two-Phase Thermodynamic model has been used to calculate the entropies of water-alcohol mixtures and ion solutions. Changes of the molar entropies are connected to the changes of the dynamics visible in the density of states.

The mixing entropy of water-methanol and water-ethanol mixtures correlates to experimental data. In water-ethanol mixtures both components contribute to the negative excess mixing entropy, in contrast to water-methanol mixtures, where the methanol molecules account for most of the entropy loss. While the rotational entropy of all molecules is lowered by mixing, the dominant contribution is always the translational entropy. The results explain the entropy loss with changes in the dynamics, but without a direct connection to the structure. No support for the “iceberg” model or molecular segregation is found. The separation in diffusive and oscillating contribution is deviates from literature, while the resulting entropies conform with earlier results. Future work could investigate mixtures of water with higher alcohols and additional inspection of the structure, to better understand the special behavior of water-alcohol mixtures.

The solvation of sodium chloride lowers the molar entropy of water, which is caused by a shift of density from diffusional motions to oscillations, that have a lower entropy. The decrease of the hydrogen bond bending peak is an effect of the superposed diffusional DoS in the interpretation of the 2PT model. The effect of larger ions on water could be investigated in future work.

Several problems of the 2PT model are illustrated. Most prominent is the use of hard sphere theory, which should not be used for the separation of the rotational DoS. Also the original method divides the number of particles in a system into two subsystems, which can not be explained physically.

Attempts were made to get rid of the empiric formulas used for the separation of the system in the diffusive and oscillating subsystem. This resulted in a new ansatz: the separation of the velocity into two components, which is mathematically not compatible with the original idea of separating the DoS. The velocity separation is in principle possible by finding and separating out the non-correlated random movement, that is superposed by the oscillating motions of each degree of freedom.

The most promising scheme to achieve this is to apply a Gaussian filter on the positional trajectory. The width of the Gaussian is increased until the smoothed out motion is free of oscillations. This scheme can be used accordingly on rotational degrees of freedom. Further investigations have to be made how good this separation scheme actually works.

The new ansatz also shows, that the split of the system in two subsystems is only physical, if it divides the systems by the kinetic energy instead of by the particle number. That changes the way the subsystems entropy is calculated. Future tests will show how well the new model performs.

Abbreviations and Symbols

Abbreviations

DoS density of states

DoF degree of freedom

VAC velocity autocorrelation function

2PT Two-Phase Thermodynamics

qHO quantum harmonic oscillator

cHO classic harmonic oscillator

MD molecular dynamics

HS hard sphere

LJ Lennard-Jones

osc oscillating

dif diffusive

trn translational

rot rotational

vib vibrational

IG ideal gas

Symbols

Symbol	Meaning
$S(\nu)$	density of states
ν	frequency
m	mass
k	Boltzmann constant
N	number of atoms
$s(\nu)$	spectral density
t	time
v	velocity
$c(t)$	velocity autocorrelation function
D	diffusion coefficient
α	Enskog friction constant
f	fluidicity factor
s_0	zero frequency value of $S(\nu)$
V	volume
T	temperature
σ^{HS}	hard sphere diameter
$z(y)$	compressibility
y	hard sphere packing fraction
Q	partition function
q	single partition function
β	$1/kT$
h	Planck constant
E	energy
S	entropy
A	Gibbs free energy
$W(\nu)$	Weighting function
E_0	2PT reference energy
ω	angular velocity
I	moment of inertia
σ	rotational symmetry number
Θ	rotational temperature
$\overline{V}$	molar volume
σ_h	LJ parameter
x	mole fraction
L	angular momentum
$\vec{e}$	eigenvector
$\vec{r}$	relative position
μ	reduced mass
ϵ	LJ parameter
P	power
$\mathscr{F}$	Fourier transform

Bibliography

[1] B. Widom, *The Journal of Chemical Physics* **1963**, *39*, 2808–2812.

[2] R. E. Nettleton, M. S. Green, *The Journal of Chemical Physics* **1958**, *29*, 1365–1370.

[3] S. Prestipino, P. V. Giaquinta, *Journal of Statistical Physics* **1999**, *96*, 135–167.

[4] M. Karplus, J. N. Kushick, *Macromolecules* **1981**, *14*, 325–332.

[5] J. Schlitter, *Chemical Physics Letters* **1993**, *215*, 617–621.

[6] F. Reinhard, H. Grubmüller, *The Journal of Chemical Physics* **2007**, *126*, 014102.

[7] S.-T. Lin, M. Blanco, W. A. G. Iii, *The Journal of Chemical Physics* **2003**, *119*, 11792–11805.

[8] S.-T. Lin, P. K. Maiti, W. A. Goddard, *The Journal of Physical Chemistry B* **2010**, *114*, 8191–8198.

[9] S.-N. Huang, T. A. Pascal, W. A. Goddard, P. K. Maiti, S.-T. Lin, *Journal of Chemical Theory and Computation* **2011**, *7*, 1893–1901.

[10] P.-K. Lai, S.-T. Lin, *RSC Advances* **2014**, *4*, 9522–9533.

[11] P.-K. Lai, C.-M. Hsieh, S.-T. Lin, *Physical Chemistry Chemical Physics* **2012**, *14*, 15206–15213.

[12] T. A. Pascal, W. A. Goddard, *The Journal of Physical Chemistry B* **2012**, *116*, 13905–13912.

[13] C. Zhang, L. Spanu, G. Galli, *The Journal of Physical Chemistry B* **2011**, *115*, 14190–14195.

[14] T. A. Pascal, S.-T. Lin, W. A. G. Iii, *Physical Chemistry Chemical Physics* **2010**, *13*, 169–181.

[15] M. P. Desjarlais, *Physical Review E* **2013**, *88*, 062145.

[16] E. R. Meyer, C. Ticknor, J. D. Kress, L. A. Collins, *Physical Review E* **2016**, *93*, 042119.

[17] T. A. Pascal, W. A. Goddard, Y. Jung, *Proceedings of the National Academy of Sciences* **2011**, *108*, 11794–11798.

[18] T. A. Pascal, S.-T. Lin, W. Goddard, Y. Jung, *The Journal of Physical Chemistry Letters* **2012**, *3*, 294–298.

[19] S.-T. Lin, P. K. Maiti, W. A. Goddard, *The Journal of Physical Chemistry B* **2005**, *109*, 8663–8672.

[20] R. F. Lama, B. C.-Y. Lu, *Journal of Chemical & Engineering Data* **1965**, *10*, 216–219.

[21] H. S. Frank, M. W. Evans, *The Journal of Chemical Physics* **1945**, *13*, 507–532.

[22] S. Dixit, J. Crain, W. C. K. Poon, J. L. Finney, A. K. Soper, *Nature* **2002**, *416*, 829–832.

[23] A. K. Soper, L. Dougan, J. Crain, J. L. Finney, *The Journal of Physical Chemistry B* **2006**, *110*, 3472–3476.

[24] D. W. McCall, D. C. Douglass, *The Journal of Physical Chemistry* **1965**, *69*, 2001–2011.

[25] R. L. Baldwin, *Biophysical Journal* **1996**, *71*, 2056–2063.

[26] Y. Zhang, S. Furyk, D. E. Bergbreiter, P. S. Cremer, *Journal of the American Chemical Society* **2005**, *127*, 14505–14510.

[27] F. Hofmeister, *Archiv für experimentelle Pathologie und Pharmakologie* **1891**, *28*, 210–238.

[28] M. A. M. Versteegh, D. Dieks, *American Journal of Physics* **2011**, *79*, arXiv: 1012.4111, 741.

[29] S. Saunders, *arXiv:1609.05504 [physics]* **2016**, arXiv: 1609.05504.

[30] H. Berendsen, D. van der Spoel, R. van Drunen, *Computer Physics Communications* **1995**, *91*, 43–56.

[31] W. L. Jorgensen, J. Tirado-Rives, *Journal of the American Chemical Society* **1988**, *110*, 1657–1666.

[32] P. H. Berens, D. H. J. Mackay, G. M. White, K. R. Wilson, *The Journal of Chemical Physics* **1983**, *79*, 2375–2389.

[33] S. v. d. Walt, S. C. Colbert, G. Varoquaux, *Computing in Science Engineering* **2011**, *13*, 22–30.

[34] M. Frigo in Proceedings of the ACM SIGPLAN 1999 Conference on Programming Language Design and Implementation, ACM, New York, NY, USA, **1999**, pp. 169–180.

[35] E. Jones, T. Oliphant, P. Peterson, et al., SciPy: Open source scientific tools for Python, [Online; accessed 2016-11-29], **2001–**.

[36] B. Veytsman, M. Kotelyanskii, Lennard-Jones potential revisited, **1997**.

[37] M. Heyden, J. Sun, S. Funkner, G. Mathias, H. Forbert, M. Havenith, D. Marx, *Proceedings of the National Academy of Sciences of the United States of America* **2010**, *107*, 12068–12073.

[38] J. D. Cox, D. D. Wagman, V. A. Medvedev, *Codata Key Values for Thermodynamics*, 1st edition, Hemisphere Publishing Corporation, New York, **1989**.

[39] A. Chandra, *Physical Review Letters* **2000**, *85*, 768–771.

Erklärung zur Master-Thesis

Hiermit versichere ich, die vorliegende Master-Thesis ohne Hilfe Dritter nur mit den angegebenen Quellen und Hilfsmitteln angefertigt zu haben. Alle Stellen, die aus Quellen entnommen wurden, sind als solche kenntlich gemacht. Diese Arbeit hat in gleicher oder ähnlicher Form noch keiner Prüfungsbehörde vorgelegen.

Darmstadt, den 16.12.2016

(Marvin Bernhardt)